UNIVERSITA' DEGLI STUDI DI NAPOLI
"FEDERICO II"

PhD Thesis in:

VETERINARY SCIENCES

(a.a. 2014-2017 XXIX CICLO)

COMBINED FUNCTIONAL, CELLULAR AND BEHAVIOURAL STUDIES TO GET INSIGHTS ON SENSORY ORGANS OF *CIONA ROBUSTA* LARVAE

Director of studies
Dr. Antonietta Spagnuolo

Author
Dr. Antonio Palladino

Index

List of Abbreviation **4**
List of Figure **5**
List of Tables **6**
Abstract **7**
Introduction **10**
1.1 Tunicates in the Chordate phylum 10
1.2 Ascidian life cycle 12
1.3 Ascidians embryonic development 13
1.4 C. robusta as a model system in embryology and developmental biology 15
1.5 The larval ascidian nervous systems 17
1.6 Generation of cell diversity in Ciona CNS: the neural plate stage 19
1.7 First aim of the thesis 23
1.8 The "eye" in Ciona 23
1.8.1 What about photoreceptor cell lineage in Ciona? 27
1.8.2 Second aim of the thesis: Gsx as a potential marker of photoreceptor cells 28
1.9 Behavioural tests on Ciona larvae 32
1.9.1 Third aim of the thesis 33
Bibliography **35**
Materials and Methods **44**
2.1 Ciona robusta eggs and embryos collection 44
2.2 Wild-type embryos for behavioral tests 44
2.3 Chemical dechorionation and in vitro fertilization 44
2.4 Transgenesis via electroporation 45
2.5 Embryos observation and imaging analyses 45
2.6 PCR amplification from genomic or plasmid DNA 46
2.7 DNA gel electrophoresis 47
2.8 DNA gel extraction 47
2.9 DNA digestions with restriction endonucleases 47
2.10 DNA dephosphorylation 47
2.11 DNA ligation 48
2.12 Bacterial cells electroporation 48
2.13 PCR screening 48

2.14 Plasmid DNA Mini- and Maxi-preparation 49
2.15 Sequencing 49
2.16 Oligonucleotides synthesis 49
2.17 Digested plasmids purification 50
2.18 Ribonucleic probes preparation 50
2.18.1 RNA labelling 50
2.18.2 Ribonucleic probes quantification by Dot Blot analysis 51
2.19 Fluorescent report assays 52
2.20 Whole Mount In situ Hybridization (WMISH) assays 53
2.20.1 Embryos preparation 53
2.20.2 WMISH protocol for single and double in situ 53
2.21 Preparation of constructs 55
2.22 In silico analysis of putative trans-acting factors 61
2.23 Chemical inhibition 62
2.24 Pressure test 63
2.24.1 Hydrostatic pressure changes 63
2.24.2 Define Interval of response 64
2.24.3 Characterize the pressure behaviour 64
2.24.4 Recording 64
2.24.5 Tracking 65
2.24.6 In vivo imaging 65
Bibliography 67
Results and Discussion 69
3.1 Generation of cell diversity in Ciona CNS: Neural Plate a-Lineage Row III Patterning 69
3.1.1 Nodal signalling and lateral patterning 69
3.1.2 Delta/Notch signaling in column 1 and 2 fates 71
3.1.3 FGF and anterior-posterior patterning of a-lineage row III 73
3.1.4 Concluding Remarks 76
3.2 Photoreceptor cells (PCRs) lineage 78
3.2.1 pGsx reporter genes to label derivatives of Gsx expressing blastomeres at the larval stage 80
3.2.2 pGsx labels PRCs territories at the larval stage 80
3.2.3 Photoreceptor territories: A-lineage or a-lineage? 81
3.2.4 Concluding Remarks 84
3.3 Behavioural tests on Ciona larvae 86
3.3.1 Does Ciona larva respond to pressure variations? 87

3.3.2 Pressure behavior characterization 87
3.3.3 Looking for structures involved into hydrostatic pressure response 88
3.3.4 GCaMP as tool to monitor neuronal activity in Ciona larvae 89
3.3.5 Concluding Remarks 92
Bibliography 94

List of Abbreviation

A–P	Anterior–Posterior
CNS	Central Nervous System
D–V	Dorsal–Ventral
EN	Endoderm
ESTs	Expressed Sequence Tags
FGF	Fibroblast Growth Factor
GRN	Gene Regulatory Network
HPF	Hour Post Fertilization
LC	Lens Cells
L–R	Left–Right
ME	Mesenchyme
MFSW	Millipore Filtered Sea Water
MO	Morpholino Oligonucleotides
MU	Muscle
NC	Nerve Cord
NICD	Notch Intracellular Domain
NO	Notochord
OC	Ocellus
OT	Otolith
PB	Posterior Brain
PCR	Polyemerase Chain Reaction
PH	Photoreceptor Cells
PRCs	Photoreceptor Cells
RPE	Retinal Pigmented Epithelium
SV	Sensory Vesicle;
TGFβ	Transforming Growth Factor Beta
TNC	Tail Nerve Cord
VG	Visceral Ganglion
WMISH	Whole-Mount *In Situ* Hybridization

List of Figure

1.1 The ascidian Ciona robusta
1.2 Phylogenetic relationships of deuterostomes
1.3 Schematic representation of the ascidian embryo at 8-cell stage
1.4 Developmental fate restriction in ascidian embryos
1.5 Schematic representation of Ciona CNS
1.6 Sensory organs in C. robusta sensory vesicle
1.7 Cell lineages of the ascidian larval CNS
1.8 Summary of the overlapping requirements of Nodal, Delta2 and FGF/MEK/ERK signalling pathways in the A-line neural plate
1.9 Schematic comparison between the main building blocks of vertebrate eye and ascidian ocellus
1.10 Schematic representation of Ciona larval trunk
1.11 Ci-gsx expression pattern during Ciona robusta development
1.12 In vivo analysis of pGsx>mCherry construct
2.1 Map of pGsx>>GFP vector
2.2 Map of pZicL/H2B/mCherry, pDMRT/H2B/YFP, pFoxB/UNC76/GFP
3.1 Expression patterns of Nodal
3.2 Nodal pattern the a-lineage CNS precursors
3.3 Expression patterns of Delta-like
3.4 Delta/Notch pattern the a-lineage CNS precursors
3.5 Effects of U0126 on Gsx endogenous transcript and its regulatory region
3.6 Effects of interference with Ets/Elk factors on Gsx endogenous
3.7 Ets/Elk binding sites on pGsx-0.39 promoter fragment
3.8 Identification of Ets/Elk binding sites on Gsx promoter
3.9 Gsx in situ analysys
3.10 Positional relationship of Gsx and FoxB gene expression
3.11 Confocal imaging of pGsx>H2BmCherry + pArr>eGFP constructs
3.12 Confocal imaging of pFoxb>H2BmChe + pArr>eGFP constructs
3.13 Confocal imaging of pArr>eGFP + pDMRT>H2BmChe constructs
3.14 Confocal imaging of pGsx>GFP + pDMRT>H2BmChe constructs
3.15 Confocal imaging of pGsx>H2BmChe + pFoxB>H2BYFP constructs
3.16 Response of Ciona larvae to pressure increase
3.17 Pressure behavior characterization
3.18 GCaMP activity in transgenic larvae
3.19 Fluorescent intensities of pTH>GCaMP
3.20 Fluorescent intensities of pTH>GCaMP
3.21 Fluorescent intensities of pTH>GCaMP

List of Tables

2.1 Genes of which ribonucleic probes have been synthesized
2.2 List of oligonucleotides used for pTH>GCaMP cloning
2.3 Oligonucleotides used for pTH>H2B>mCherry cloning
2.4 Mutagenic oligonucleotides

Abstract

The ascidian *Ciona robusta* is a powerful model system to approach in a "simple context" cellular, developmental, and behavioral strategies that have been adopted in the lineage of chordates. In particular, the simplicity of *Ciona* CNS (Central Nervous System) permits to follow the fate of each blastomere from neural plate up to the larval stage, thus representing a huge advantage compared to the thousands of cells present in vertebrates. Furthermore, the lineage specific promoters collected by ascidian community in the last years, coupled with the technique of transgenesis through electroporation, permit to label unique or small groups of cells in the developing CNS and visualize them in their final differentiated state in swimming larvae. In the course of my thesis studies, I have exploited all these advantages to study early developmental mechanisms guiding the correct specification of blastomeres of a-lineage row III, the anterior part of neural plate that gives rise to most of the structures of the sensory vesicle of the larva. By transgenesis and chemical inhibition experiments, I have proved the involvement of three signaling pathways, Nodal, Delta-like/Notch and FGF, in the activation of three markers, *Tyrp, Gsx* and *Meis*, specific of each blastomere pairs of a-lineage row III. As further step, I have demonstrated a direct transcriptional control of FGF signaling on one of these markers, the Para-Hox transcription factor *Gsx*. Interestingly, *Gsx* has been instrumental also for the continuation of my studies, since, at later stages of development, it revealed to be a useful marker also for photoreceptor cells differentiation up to the larval stage. The data on this part of work further support the evidences, previously collected by the former PhD student of the Lab, on the involvement of *Ciona Gsx* in the developmental programs leading to photoreceptor cells differentiation, which opens new perspectives about the function of this transcription factor in nervous system formation during evolution.

In the last part of my PhD studies, I spent three months in Gaspar Jekely lab, at the Max Planck Institute for developmental biology, to explore the possibility of *Ciona* larva to sense hydrostatic

pressure changes. My experiments showed for the first time that *Ciona* is able to sense pressure increases by swimming faster upward during a precise developmental window after hatching. Furthermore, I have tested the potential involvement of coronet cells, a group of cells close to the group III photoreceptor cells present in the sensory vesicle, as candidate for pressure detection. These experiments indicated that coronet cells are not involved in pressure perception but, may be, could play a role in the modulation of photic response.

Chapter 1

Introduction

The model organism: the ascidian *Ciona robusta*

1.1 Tunicates in the Chordate phylum

The word "model" has many meanings but, in science, a model organism is a simplified system, either animal, plant or microbe, that can help to understand the basic operating principles governing biological processes. Thanks to model organisms, researchers have identified, for example, the fundamental properties of how cells grow and divide, how inheritance works, how organisms store and use energy and, more recently, a huge number of information are being gathered on the mechanisms by which gene regulatory networks (GRN) operate during development and how GRN have emerged during evolution.

During my PhD I have conducted my studies on the ascidian model system *Ciona robusta* (previously named *Ciona intestinalis*) (Brunetti, 2015).

Ascidians, or sea squirts, are sessile marine invertebrate chordates ubiquitous throughout the world; they have been recognized since the ancient Greeks and described firstly by Aristotle. In fact, the name "ascidian" originated from the Greek word *askidion*, meaning a small bag because of their soft bodies. They were initially included among the molluscs by Carl Linnaeus, based on their adult form (Linnè, 1767).

Only in 1886, the great Russian embryologist Alexander Kowalevsky discovered that the ascidian larva has the general appearance of a simplified vertebrate tadpole, by possessing a notochord and a dorsal neural tube and this provided clear evidence that ascidians are, along with vertebrates and the cephalochordate amphioxus, members of the phylum Chordata. The adult ascidian also possesses recognizable chordate features, even though it is a sedentary filter-feeder animal and is more divergent than the larva. The feeding basket of the adult, indeed, contains gill slits that appear to share a common origin with the gill slits of other chordates (Aros and Viragh, 1969). Likewise, the endostyle of the adult ascidians is considered to be homologous of the vertebrate thyroid gland,

sequestering iodine and producing thyroid hormone (Eales, 1997) (Fig. 1.1).

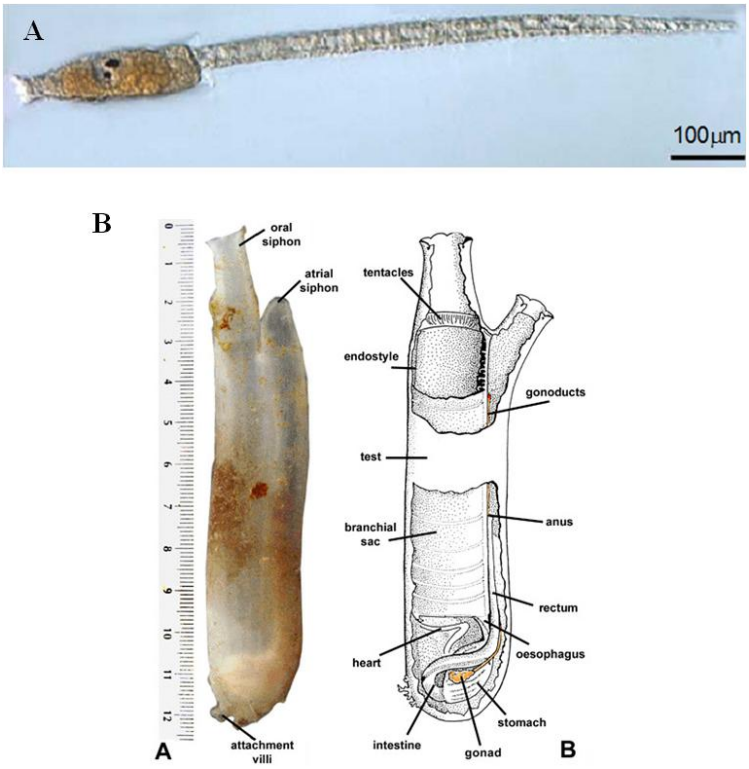

Fig. 1.1 The ascidian Ciona robusta. A. *Tadpole larva.* ***B.*** *Adult.*

The chordata phylum comprises three subphyla: urochordata (or tunicata), cephalochordata and vertebrata. Studies based only on morphological observations initially stated that cephalochordates are the closest living relatives of vertebrates, whereas tunicates were placed in a more basal evolutionary position (Beaster-Jones et al., 2008; Schubert et al., 2006). More recently, accurate studies by Delsuc, involving phylogenomic data set of 146 nuclear genes from 14 deuterostomes and 24 other slowly evolving species as an outgroup, demonstrated that "Tunicates and not Cephalochordates are the closest living relatives of Vertebrates" (Capellini et al., 2008; Delsuc et al., 2006; Putnam et al., 2008; Vienne and Pontarotti, 2006) (Fig. 1.2).

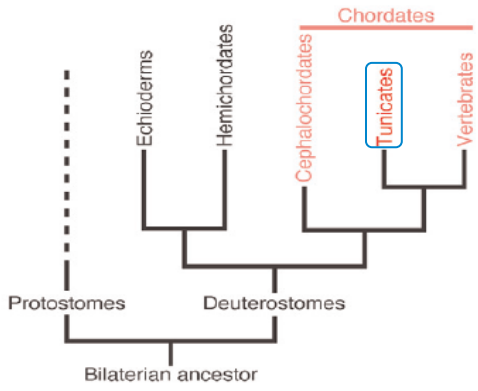

Fig. 1.2 Phylogenetic relationships of deuterostomes. *Ascidians belong to Tunicates subphylum (blue circle). (Adapted from Sasakura et al., 2007).*

The Urochordata or Tunicata subphylum comprises three classes: ascidians (sea squirts), thaliaceans (salps) and appendicularians (larvaceans). All animals from these different classes share the presence of a tunic that covers their entire body, from which the subphylum name, Tunicata, is derived. The major constituent of the tunic is a type of cellulose, the tunicin. Tunicates are the only animals that can synthesize cellulose independently (Brusca, 2003).

1.2 Ascidian life cycle

C. robusta life cycle is relatively rapid. In fact, eggs develop into adults with reproductive capacity within 2–3 months, or earlier in warm waters, suggesting that under optimal conditions *Ciona* can pass through several generations within a year. The fully developed, hatched *Ciona* larva actively swims, for one or two days, before settling on the substrate and initiating metamorphosis (Svane, 1989). During this free-swimming period, the larva displays a characteristic pattern of behaviour, initially swimming upward (toward surface to help to be dispersed), then starts swimming downward (away from illuminated water surface) to find suitable substrates to attach and start metamorphosis (Svane, 1989). After metamorphosis, the swimming larva passes throughout a sessile juvenile stage before becoming adult.

1.3 Ascidians embryonic development

The main reason why ascidians have long attracted embryologists is their relative embryonic simplicity compared to vertebrates. *Ciona* eggs are 130–150 μm in diameter and are enclosed by a non-cellular vitelline coat or chorion. On the outer surface of the vitelline coat are attached follicle cells, while many test cells are present within the space between the egg and the vitelline coat. The existence of test cells within the space is a unique phenomenon in the animal kingdom. Test cells are likely to be involved in oogenesis and in the formation of the larval tunic (Satoh, 2003). After fertilization, the cleavage of ascidian eggs is invariant and bilaterally symmetrical. The first plane divides the right and left halves; the second cleavage plane, perpendicular to the first one, lead to the formation of four blastomeres usually of equal sizes. After the third cleavage, the four upper cells lie slightly anterior to the four lower cells. Thus, from the 8-cell stage onward, the A–P (anterior–posterior), D–V (dorsal–ventral), and L–R (left–right) axes become evident. An outstanding feature of ascidian embryogenesis is that the developmental fates of embryonic cells are restricted at very early stages, since the 8-cell stage, when the embryo consists of the founder cells of four lineages, with the cells of the vegetal pole indicated by capital letters, A4.1 and B4.1, and animal cells named with small letters, a4.2 and b4.2 (Fig. 1.3) (Conklin, 1905).

The embryo continues the cleavages in a bilaterally symmetrical manner and thus each blastomere name refers to a pair. The timing of cell division becomes asynchronous after the 16-cell stage, temporarily resulting in 44-cell and 76-cell embryos. From the fourth to the seventh cleavage, the posterior-most vegetal cells divide unequally, producing smaller daughter cells positioned posteriorly. Divisions of the animal blastomeres are synchronous, reflecting the clonal organization of ectodermal cells. By contrast, the vegetal blastomeres have different temporal division patterns, and these cells give rise to various tissues of mesodermal and endodermal origin.

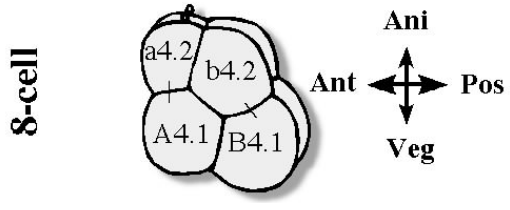

Fig. 1.3 Schematic representation of the ascidian embryo at 8-cell stage. *Anl: Animal pole; Veg: Vegetal pole; Ant: Anterior; Pos: Posterior*

As early as the 16-cell stage, a pair of epidermis-restricted cells (b5.4 pair) appears in the animal hemisphere. Then, at the 32-cell stage, two pairs of cells in the vegetal hemisphere (A6.1 and B6.1 pairs) become restricted to endoderm. By the 64-cell stage, blastomeres appear restricted to their various individual fates: notochord, muscle, mesenchyme, and, by the 112-cell stage, fate restriction is accomplished in 102 over 112 blastomeres (Fig. 1.4) (Satoh, 2014). Gastrulation starts at 112-cells stage when endodermal and mesodermal cells of the vegetal hemisphere ingress into the interior while the ectodermal layer migrates toward the vegetal pole to envelope the embryo. The spatial relationships among cells derived from the vegetal hemisphere are basically retained during these morphogenetic cell movements. Neural plate formation initiates before the completion of blastopore closure. The neural plate consists of distinctly arranged rows of cells. As in vertebrates, *Ciona* CNS develops via neurulation, which begins with the formation of the neural plate and ends when the left and right epidermis overlying the neural tube fuse to close the neural fold. The formation of this tube-like structure progresses from posterior to anterior. Once it is completely closed, the tail becomes elongated.

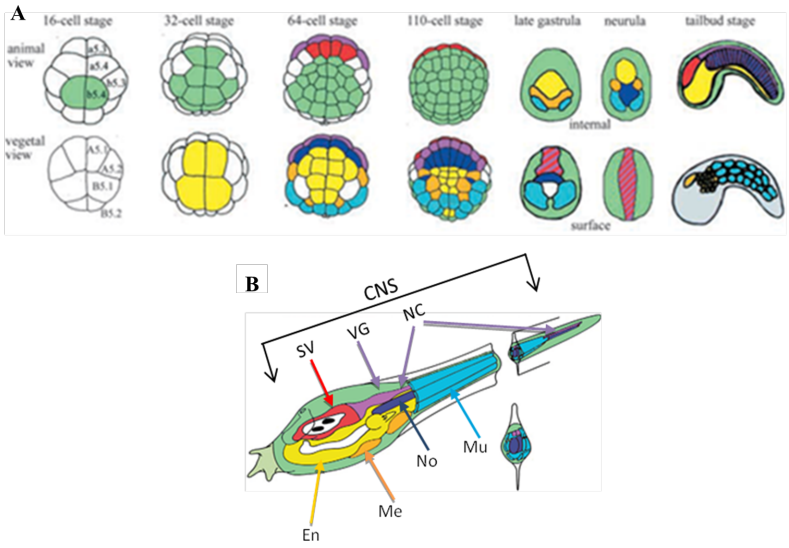

Fig. 1.4 Developmental fate restriction in ascidian embryos. A. *Schematic representation of the ascidian embryo from 16-cell stage to tailbud stage. Blastomeres whose developmental fate is restricted to one tissue are in color: yellow (endoderm); orange (mesenchyme); light blue (muscle); dark blue (notochord); green (epidermis); light purple (nerve cord); red (nervous system).* ***B.*** *Schematic overview of the major tissue types in Ciona robusta tadpole larva. The color code is the same as in A. Light green: palps. SV: sensory vesicle; VG: visceral ganglion; NC: nerve cord; En: endoderm; Me: mesenchyme; No: notochord; Mu: muscle. (Adapted from Imai et al., 2004 and Munro et al., 2006).*

Upon tailbud formation, the embryo enters the tailbud stage, during which the tail continues to elongate until the embryo is ready to hatch. The metamorphosis of tadpole-like swimming larvae to sessile juveniles and adults involves dynamic and complex changes in the shape and physiology of tissues. It takes 2 or 3 months for the juvenile to become adult with reproductive capability, depending on the temperature of the environment (Marikawa et al., 1994).

1.4 *C. robusta* as a model system in embryology and developmental biology

C. robusta has represented, for over a century, a choice organism for experimental biology (Chabry, 1887; Conklin, 1905; Morgan, 1923) and, more recently, it has emerged as a powerful popular organism in developmental biology, in particular to investigate the molecular mechanisms underlying cell-fate specification during chordate development. The reason of this success is related to a number of advantages that *Ciona* offers for this type of studies. First of all *Ciona* embryo develops rapidly, with the tadpole larva completing development in 18 hr when reared at 18°C (Whittaker, 1977). Furthermore, the cleavage program of the embryo is invariant and accurate fate maps have been

drawn to trace the embryonic development (Conklin, 1905; Ortolani, 1964; Nishida, 1987). When fully developed, *Ciona* larva is relatively simple, being composed of only 2,500 cells (Satoh, 2001), and contains only six types of tissues/organs: the epidermis, the central nervous system (CNS), the endoderm and mesenchyme in the trunk, and the notochord and muscle in the tail (Fig. 1.4B) (MJ., 1983).

At the larval stage, the notochord is composed of only 40 cells; the muscle of 36 cells and the CNS of 350 cells, of which 100 are neurons (Nicol and Meinertzhagen, 1991; Satoh, 2001). This small number of cells allows the investigation of the molecular mechanisms underlying cell differentiation and morphogenesis almost at the single-cell level. *Ciona* embryos and larvae are transparent, permitting a direct observation of tissues without need for sectioning.

C. robusta genome, fully sequenced (Dehal et al., 2002) is around 117-Mb and the extimated presence of around16000 protein-coding genes means that one gene occupies 7.7 kb on average. *Ciona* is one of the animals for which the most through cDNA information has been accumulated (Satou and Satoh, 2005; Satou et al., 2002). A total of 1,205,674 expressed sequence tags (ESTs), at different developmental stages, has been registered in the National Center for Biotechnology Information (NCBI) database of expressed sequence tag (dbEST) database. Over 6700 full-length cDNA sequences are available in the DDBJ/GenBank/EMBL databases and 13,464 unique cDNA clones have been obtained.

Ciona genes are organized in the genome more compactly than those of the protostomes (except *Caenorhabditis elegans*), deuterostomes, and vertebrates. As a consequence of that, most of the promoters are relatively short and usually located in close proximity, within the first 1.5 kb upstream, of the transcription start site of the genes (Alfano et al., 2007; Corbo et al., 1997; Fanelli et al., 2003; Squarzoni et al., 2011; Takahashi et al., 1999). In addition, the genome of *Ciona savignyi*, a closely related species of *C. robusta*, has also been sequenced and comparisons between complementary *C. robusta* and *C. savignyi* sequences have indicated that these two species are at sufficient evolutionary

distance to permit efficient identification of conserved regulatory sequence information (Bertrand et al., 2003; Johnson et al., 2004; Squarzoni et al., 2011). These peculiarities, combined with the method of transgenesis by electroporation, that permits the transformation of hundreds or even thousands of embryos simultaneously (Corbo et al., 1997) have made *Ciona* particularly useful for studies of transcriptional regulation. This technique allows also to create ‘‘knock-out’’ phenotypes by expressing dominant negative forms of genes of interest using lineage-specific enhancers (Christiaen et al., 2009; Squarzoni, 2011). Gene function can be tested also by microinjection of antisense morpholino oligonucleotides (MOs) and, owing to the fast pace of ascidian embryogenesis, results can be obtained within one or two days (Christiaen et al., 2009). Recently targeted knock-down methods such as TALEN (Treen et al., 2014) and CrispR-Cas9 (Sasaki et al., 2014; Stolfi et al., 2014) have been developed.

Thus, all these features, coupled with a simplified chordate body plan that contains rudiments of most vertebrate tissues, make *Ciona* a very suitable model organism to explore the genetic circuitry responsible for the establishment of the typical basic chordate body plan, such as the development and compartmentalization of the nervous system.

1.5 The larval ascidian nervous systems

Morphologically the ascidian larval CNS is divided into five major parts along the A–P axis: the brain or sensory vesicle (SV), the neck, the visceral (motor) ganglion (VG), and the tail nerve cord (TNC) (Lemaire et al., 2002; Meinertzhagen et al., 2004; Meinertzhagen and Okamura, 2001) (Fig. 1.5). These regions are thought to correspond to the vertebrate forebrain (SV), midbrain–hindbrain boundary (Capellini et al.), hindbrain (VG) and spinal cord (TNC), respectively (reviewed in Lemaire, 2002) (Dufour et al., 2006).

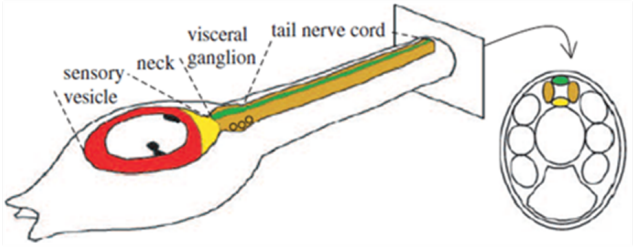

***Fig. 1.5 Schematic representation of Ciona CNS**. The section highlights the four rows of ependymal cells present in the tail nerve cord.*

The tadpole larva has a fairly simple brain distantly related to our own but made up of only about 330 cells, of which about 100 cells are presumed to be neurons and the others ependymal glia cells, on the basis on their cytological appearance (Cole and Meinertzhagen, 2004; Nicol and Meinertzhagen, 1991).

More recently, a deep study conducted by Ryan (Ryan et al., 2016) using serial-section at electron microscopy, revealed that the larval brain contains more than 100 neuron, precisely 177. These can be split into at least 25 types and each neuron has a simple, mostly unbranched shape with, on average, 49 synapses with other cells. Thus, even though it has such a small number of neurons, the neuron network is still relatively complex.

Ciona SV contains two conspicuous pigmented sensory organs (Fig. 1.6).

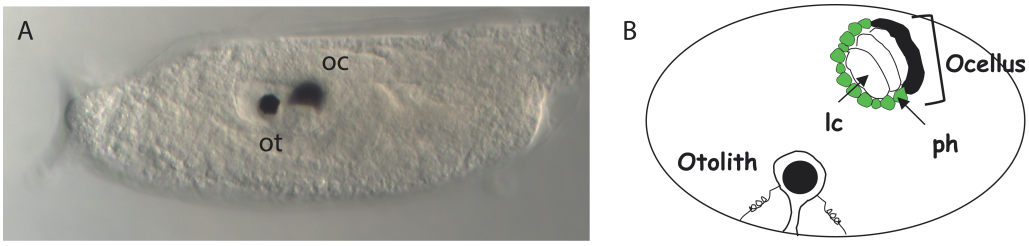

***Fig. 1.6 Sensory organs in C. robusta sensory vesicle. A.** Larval trunk. Anterior is on the left. **B.** Schematic representation of the pigment sensory organs in the sensory vesicle. The pigment cells of the otolith (ot) and of the ocellus (oc) are represented in black. lc: lens cells; ph: photoreceptor cells.*

The pigmented sensory organ located anterior is the otolith, used for the perception of gravity, and the posterior one is the ocellus, used for light reception (Sakurai et al., 2004; Tsuda et al., 2003b) (Fig. 1.6). The otolith is a spherical mass of pigment granules connected to the midline of the floor of SV by a narrow stalk (Eakin and Kuda, 1971; PN., 1969; Sakurai et al., 2004). The otolith-associated

neurons extend their axon to the posterior brain (Horie et al., 2008b).

Ciona ocellus is composed of three lens cells, one pigmented cell, and about 30 photoreceptor cells (PRCs) (Eakin and Kuda, 1971; Horie et al., 2005, Horie, 2008 ; Nicol and Meinertzhagen, 1991; PN., 1969).

Sensory neurons in the SV, including the ocellus photoreceptor cells and the otolith cell, project to the PB (Horie et al., 2005; Horie et al., 2008b). Epidermal sensory neurons also project to the PB (Horie et al., 2008b). Thus, many axon terminals of sensory neurons arrive in the PB. Some interneurons in the PB form synaptic connections within the PB, and others send axons posteriorly to the VG (Horie et al., 2008b; Imai and Meinertzhagen, 2007; Yoshida et al., 2004). Collectively, it appears that the PB may be a processing center able to integrate sensory inputs and control the motor system (Horie et al., 2008b).

The visceral ganglion contains motor neurons that innervate the tail (Imai and Meinertzhagen, 2007; Meinertzhagen and Okamura, 2001; Okada et al., 1997; Okada et al., 2002; Q., 1992). The tail nerve cord (Fig. 1.5) consists of four rows of ependymal cells: right and left lateral cells, and dorsal and ventral cells (Crowther and Whittaker, 1992).

1.6 Generation of cell diversity in *Ciona* CNS: the neural plate stage.

The CNS derives from three of the four blastomere types present at the eight-cell stage, the a-, b and A-blastomeres (Fig. 1.3) that cleave in a bilaterally symmetrical manner so that each blastomere name refers to a pair. Patterning of CNS starts during gastrulation when it is arranged as a neural plate showing a grid-like organization. The neural plate is made of 44 cells in total, 24 coming from a-line, 14 from A-line and 6 from b-line, arranged in six rows of cells along the A-P axis, and three bilateral pair of columns in which the medial identified as columns 1, the intermediate as column 2 and the lateral as column 3. The posterior rows I and II derive from A-lineage while the anterior rows III-VI are from the a-lineage (Fig. 1.7 A, B). Despite its simple organization, the neural plate is

highly compartmentalized. Posterior A-line row I and II, indeed, give rise to the more posterior regions of the CNS (posterior sensory vesicle, visceral ganglion, lateral and ventral rows of ependymal cells in the tail). The anterior a-line rows III e VI generate parts of the sensory vesicle and contribute to the oral siphon primordium (Christiaen et al., 2007; Cole and Meinertzhagen, 2004; Nishida, 1987), while the most anterior a-line rows V and VI form a specialized region of the anterior epidermis (Fig. 1.7), including a placode-like territory and the palps (Abitua et al., 2015; Nishida, 1987).

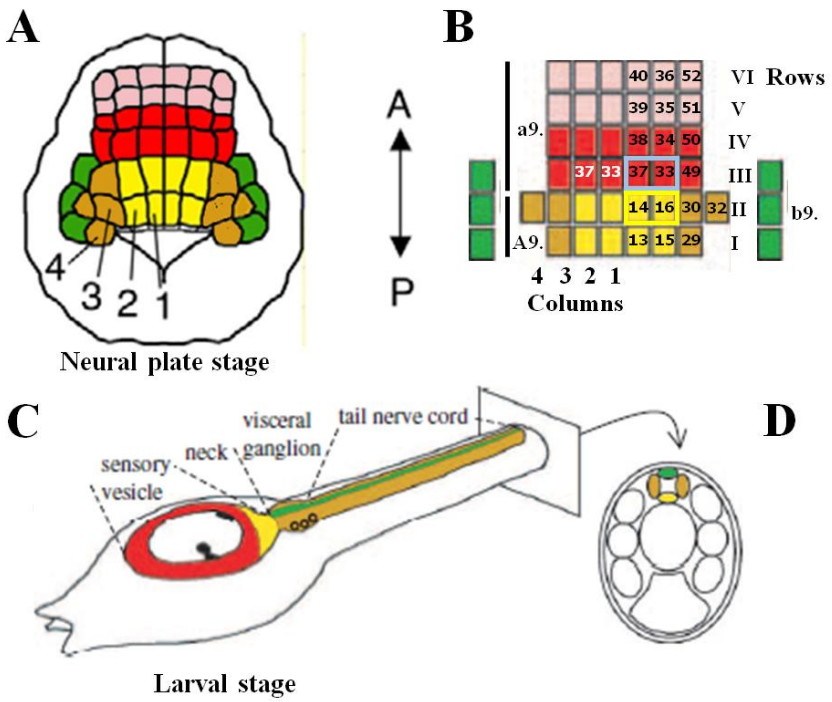

Fig. 1.7 Cell lineages of the ascidian larval CNS. *Schematic representation of Ciona neural plate stage (A), neural plate (B), larval stage (C) and section of the tail nerve cord to show the four rows of ependymal cells (D). Cell lineages are indicated as follows: the a-line is coloured red (anterior sensory vesicle precursors) or pink (anterior epidermis and pharynx/neurohypothesis precursors); b-line is green and A-line light yellow (medial cells) or tan (lateral cells). Light blue rectangle in B indicates the former lineage of photoreceptor cells (right a9.33, a9.37 cells), yellow rectangle in B indicates the revised lineage of photoreceptor cells (right A9.14, those of the pigmented ocellus, right A9.16 those of the non- pigmented ocellus). Supposed precursors of coronet cells (left a9.33 and a9.37 blastomeres) are indicated in white.*

The fate of each pair of cell in the neural plate is accomplished by a unique combination of transcription factors and signaling pathways, as Nodal, Delta-Notch and FGF, that act on them. Nodal pathway involves binding of Nodal protein (a subset of the transforming growth factor beta (TGFβ)

superfamily) to activin and activin-like receptors. This interaction leads to phosphorylation of Smad proteins and their translocation into the nucleus where Smads interact with specific transcription factors, such as FoxH1, p53, Mixer, leading to the formation of active transcription complexes on target promoters (Germain et al., 2000; Randall et al., 2004).

In the Notch-Delta signaling, Notch is a cell-surface receptor that transduces short-range signals by interacting with transmembrane ligands such as Delta on neighboring cells. Ligand binding leads to cleavage and release of the Notch intracellular domain (NICD), which then travels to the nucleus and cooperates with DNA-binding protein, as CBF1, Su(H), LAG-1 and its coactivator Mastermind (Treen et al.) to promote transcription (reviewed by Bray, 2006).

FGFs are secreted ligands that through the binding to a class of receptor tyrosine kinases, the FGF receptors (FGFRs), predominantly activate the Ras/MEK/ERK cascade (reviewed by Szebenyi, 1999) that leads to phosphorylation of FGF downstream effectors, as the well-known Ets family members of transcription factors (Wasylyk et al., 1998).

In a previous study, using a combination of morpholino gene knockdown, dominant-negative forms and pharmacological inhibitors, Yasuo group (Hudson et al., 2007) demonstrated that Nodal signaling is required, at around 64- to 76-cell stage, for the formation of all lateral A-line (rows I and II) neural plate fates of columns 3 and 4. This effect is accomplished through the activation of Delta2 and Snail, two early transcriptional targets of Nodal signaling both expressed at early gastrula stages in the precursors of columns 3 and 4 (Corbo, 1997; Hudson, 2005; Wada, 1999). In this scenario, Delta2, acting as activator through interaction with Notch receptor, is responsible for the formation of lateral A-line in rows 1 and 2 (column 4 versus 3 and column 2 versus 1). On the other hand, Snail, acting as repressor, is largely responsible for the repressive function of Nodal signals, being required and sufficient to repress A-line medial fates (Hudson et al., 2015).

Simultaneously, FGF signalling establishes antero-posterior identities in A-line lineages, through a

differential activation of ERK1/2 between rows I-II, in a way that activated ERK1/2 promotes row I fates and represses row II fate.

Thus, collectively, each A-line cell, present on both sides of the bilaterally symmetrical embryo, receives a unique combination of these three signalling pathways (Fig. 1.8), which determines the eight distinct cell types (Hudson et al., 2007).

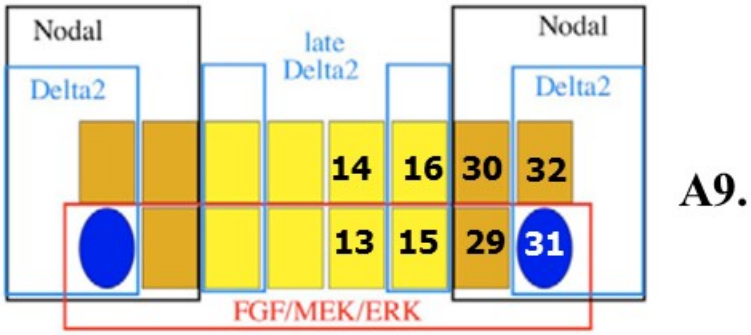

Fig. 1.8. *Summary of the overlapping requirements of Nodal, Delta2 and FGF/MEK/ERK signalling pathways in the A-line neural plate. A-line lineages are shown in yellow for medial precursors and tan for lateral precursors, with the secondary muscle precursor colored in blue (From Hudson et al. 2007).*

Like in the A-lineage derived neural plate, differential FGF/ERK signalling also patterns the a-lineage derived neural plate along its anterior-posterior axis. Specifically, FGF/ERK signalling is required to promote row III over row IV cell identities (Haupaix et al., 2014; Racioppi et al., 2014; Squarzoni et al., 2011).

Similarly, like in the A-lineage neural plate, Nodal signalling is implicated in specification of the lateral part of the a-lineage neural plate, as lateral gene expression is lost in the a-lineage cells when Nodal signalling is inhibited (Hudson and Yasuo, 2005; Imai et al., 2006; Ohtsuka et al., 2014).

1.7 First aim of the thesis

At the time I started my PhD in the BEOM Laboratory at the SZN, the research group I joined, led by Antonietta Spagnuolo, was just studying, in collaboration with Dr. Clare Hudson and Dr. Hitoyoshi Yasuo (Obstervatoire Océanologique in Villefranche sur mer), the molecular mechanisms involved in the patterning of row III a-lineage.

This study was conducted by using a number of interference approaches, as morpholino injection, expression of dominant-negative forms and pharmacological inhibitors, in combination with the analysis of the expression of a set of three marker-genes, *Trp*, *Gsx* and *Meis*, which label row III cells in columns 3 (lateral), 2 (intermediate), and 1 (medial) respectively, at neurula stages. **As first aim of my PhD thesis,** I thus contributed to this study by analysing the expression pattern of the three marker genes in "interfered" *Ciona* embryos. In a next step, I devoted my efforts to the demonstration of a direct relation between early activation of one of these markers, *Gsx*, and the inputs generated by FGF signalling in *Ciona* row III neural plate. To this end, I conducted a series of systematic mutation analyses, by exploiting the Gsx minimal promoter, previously isolated in the Laboratory.

1.8 The "eye" in *Ciona*

The eye, in vertebrates is a complex optical system which collects light from the surrounding environment, focuses it through an adjustable assembly of lenses to form an image, converts this image into a set of electrical signals, that are transmitted to the brain through intricate neural pathways. Despite its complex function and structure, the main building blocks of vertebrate eye are two: the neural retina and the RPE (Retinal Pigmented Epithelium; Fig 1.9). The retina contains the photoreceptor cells devoted to perceive light and convert it into signals; the RPE is a monolayer of pigmented cells that closely interacts with photoreceptors and, among a number of roles, is involved in the maintenance of visual function and in protecting photoreceptors from excess incoming light.

In comparison with vertebrate eye, the simplest "eye", such as *Ciona* ocellus, is only able to detect whether the surroundings are light or dark; nevertheless, its building blocks are two, as in vertebrates: the photoreceptor cells and the dark shielding pigment cell (Fig 1.9 B).

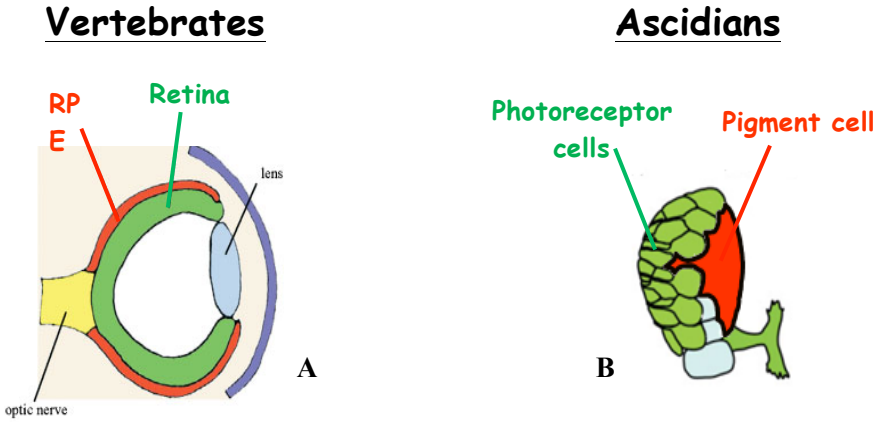

Fig 1.9 Schematic comparison between the main building blocks of vertebrate eye (A) and ascidian ocellus (B). *Retinal Pigmented Epithelium of the eye (A) and pigment cell of the ocellus (B) are depicted in red. Retina of vertebrate eye (A) and photoreceptor cells of the ocellus (B) are depicted in green.*

A relatively recent study (Horie et al., 2008a) showed that *Ciona* larva has three morphologically distinct types of photoreceptor cells in the SV, defined as group I, group II, and group III photoreceptor cells (Fig. 1.10).

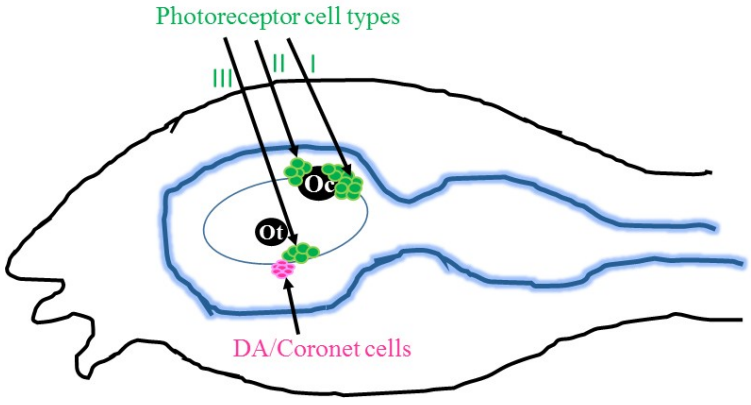

Fig. 1.10 Schematic representation of Ciona larval trunk *to show location of photoreceptor cell types and coronet cells. Ot and Oc: Otolith and Ocellus pigment cells.*

The group I photoreceptor cells (18-23 cells) are those traditionally recognized as the ocellus photoreceptor cells in ascidian larvae. The group II and group III photoreceptor cells represent instead two novel types of photoreceptor cells, never reported before in any ascidian species. The group II photoreceptor cells (8-11 cells) are associated, as the group I, to the ocellus pigment cell. However, while the group I have outer segments arranged in rows inside the pigment cup of the ocellus, the group II are located outside of the pigment cup, directly exposed to the lumen of the sensory vesicle. The group III photoreceptor cells constitute a novel ocellus lacking a pigment cell and consisting of a little group of photoreceptor cells (6 or 7), located in the left ventral part of the sensory vesicle, in proximity to the otolith and apart from the ocellus pigment cell. In this case, the outer segments exposed into the lumen of the sensory vesicle present a peculiar circular shape. Accordingly, the ascidian larva has two ocelli: a 'conventional' pigmented ocellus containing the group I and group II photoreceptor cells and a novel non-pigmented ocellus consisting of the group III photoreceptor cells. In close relationship with the group III of photoreceptors, a cluster of dopamine (DA)-synthesizing putative sensory neurons, the so-called coronet cells (Fig. 1.7), is present (Eakin`and Kuda, 1971; Nicol`, 1991; Moret, 2005a). The function of these cells is not clear yet. Several authors (Eakin and Kuda, 1971; PN., 1969) speculated roles in pressure detection (hence the name of pressure organ), but these hypotheses seem not supported by experimental data (Tsuda et al., 2003b). On the other hand, more recently, a role of these cells in the modulation of the photic response has been suggested by Razy-Krajka and colleagues (Razy-Krajka et al., 2012).

It is intriguing to note that some aspects of photo-transduction and developmental mechanisms of *Ciona* ocellus appear to be shared with vertebrate eyes, thus indicating that these two structures could have been derived from a common archetypal "visual organ" (Kusakabe et al., 2001; Sato and Yamamoto, 2001; Lamb et al., 2007).

In particular, the light-response of *Ciona* photoreceptors is hyperpolarizing and ciliary, as for vertebrates (Gorman et al., 1971). Furthermore, the photo-transduction process in vertebrates requires

the visual opsins, which are G-protein coupled receptors, and visual arrestins, small proteins needed to regulate opsin signal transduction (Arshavsky, 2002; Blomhoff and Blomhoff, 2006). Similarly, photo-transduction in *Ciona* uses opsins, precisely Ci-opsin1 (three opsin homologs are present in *Ciona* genome) and Ci-arrestin (one arrestin homolog is present in *Ciona* genome), both expressed in ocellus photoreceptor cells as well as in the group III of photoreceptor cells (Kusakabe et al., 2001; Nakagawa et al., 2002; Nakashima et al., 2003; Horie et al., 2008b).

The "visual systems" of *Ciona* share with vertebrates also some similarities at molecular-developmental level.

As an example, it is known that in vertebrates Pax6 is involved in eye formation. Mutations in vertebrate and invertebrate *Pax6* gene result in defects or absence of the eye (Callaerts et al., 1997). In tunicates Pax6 is expressed in the nervous system territories, including pigment organ precursors, but its role has not been clarified yet (Mazet et al., 2003). However, it has been demonstrated that the ectopic expression, in *Drosophila* imaginal discs, of *Pax6* homologous genes, from either the ascidian *Phallusia mamillata*, mouse or *Drosophila*, causes the formation of supernumerary eye structures, indicating a functional conservation among different species (Halder et al., 1995; Glardon et al. 1997). In addition, *Ciona Ci-Rx*, as its vertebrate homologous gene *RX*, are both required for ocellus/eye formation and function (Bailey et al., 2004) (D'Aniello et al., 2006). As a further link between ocellus and eye, in *Ciona* ocellus are expressed homologs of three vertebrate proteins that are involved in the retinoid cycle of vision: RPE65, CRALB P and BCO (Takimoto et al., 2006). Finally, the melanogenic enzymes Tyrosinase and TRPs are expressed in vertebrate RPE as well as in tunicate pigment cells and their precursors (del Marmol and Beermann, 1996; Caracciolo et al., 1997; Sato et al., 1997; Esposito et al., 2012).

Collectively, all these data strongly support *Ciona* as a valuable model system to study, in a relatively simple way, the "basic" mechanism underlying the development of complex structures, such as the eyes, much more difficult to be approached in vertebrates. *Ciona* model system, indeed, permits in

most cases to depict precisely the lineage of the tissue/structure of interest and, at the same time, identify a gene, or group of genes, that specifically labels these territories since early stages of development.

1.8.1 What about photoreceptor cell lineage in *Ciona*?

As previously mentioned, in *Ciona* extensive information are available on the cell lineage of most of the main tissues and organs, so that it is possible to follow many developmental processes. Concerning the lineage of photoreceptor cells, a detailed analysis of the mitotic history of CNS precursor cells led to infer that, since neural plate stage, the right a9.33 and a9.37 cells most probably represent the photoreceptor cell progenitors (Cole and Meinertzhagen, 2004; Nicol and Meinertzhagen, 1991) (Fig. 1.7 B light blue rectangle).

In the same study Cole and Meinertzhagen (2004) inferred that some of the progeny from left a9.33 and a9.37 blastomeres (Fig. 1.7 B white characters) likely forms the almost 20 coronet cells, which lie in proximity to the otolith and close to the group III of photoreceptors (Cole and Meinertzhagen, 2004). Interestingly, the fate map of photoreceptor cells has been revised in 2015 (Gainous et al., 2015), when the authors provided evidence that photoreceptor cells may be derived from more posterior regions of the neural plate, most likely medial regions of row II. This data has been further confirmed by a very recent and detailed study, in which the authors traced the developmental fates of neural plate cells from the late gastrula through larval stages by labelling particular cells of "non dechorionated" embryos at single-cell resolution using Kaede photoactivable reporter. Their results indicated that the photoreceptor cells of both ‘conventional’ pigmented ocellus, containing the group I and group II, and of non-pigmented ocellus, consisting of the group III photoreceptor cells, develop from the right anterior vegetal hemisphere (A-lineage). Specifically those of the pigmented ocellus are from the right A9.14 cell and those of the non-pigmented ocellus are from the right A9.16 cell (Fig. 1.7 B yellow rectangle).

1.8.2 Second aim of the thesis: *Gsx* as a potential marker of photoreceptor cells

Gsx, together with Xlox and Cdx, belongs to the ParaHox family of transcription factors, considered the paralogue of the Hox genes (Brooke et al., 1998). As the name suggests, both ParaHox belong to the homeobox family, an ancient group of genes characterized by the presence of a DNA sequence, the homeobox, which codes for the homeodomain. The homeodomain is the peptide motif that actively binds the DNA and it is constituted by 60 amino acids arranged into a recognizable helix-turn-helix structure (McGinnis et al., 1984; Scott and Weiner, 1984; Lewin, 2000). Most homeodomain proteins bind to short DNA sequences of only 6 bp, often with a common TAAT core followed immediately by two bases that confer specificity (Treisman et al., 1989, 1992).

Among the Hox/ParaHox gene families, *Gsx* is one of the most conserved throughout the animal kingdom, with orthologues found from placozoans up to vertebrates. Studies aimed at the reconstruction of its function and diversification during evolution are facilitated by the relatively conservative history of *Gsx*, without intensive duplication events (Finnerty et al., 2003). The sole duplication event occurred in the vertebrate lineage, before the divergence of bony fishes and tetrapods, giving rise to two paralogs, *gsh-1* and *gsh-2* (Hsieh-Li et al. 1995; Valerius et al. 1995; Deschet et al. 1998). Phylogenetic studies revealed the presence of a *Gsx* ortholog, *trox2*, even in the placozoan *Trichoplax adherens*.

In *Cnidaria phylum,* the first *phylum* provided with a well differentiated nervous system, one Gsx ortholog, called *cnox2,* has been characterized (Finnerty et al., 2003).The role of *cnox2* was elucidated, thanks both to expression and functional studies, and the results showed that gsx/cnox2 function is related to neurogenesis and oral patterning. Referring to this, in *Hydra* it has been clearly demonstrated that cnox2, marking specifically the nervous system, promotes apical neurogenesis and head patterning during head regeneration after amputation (Miljkovic-Licina et al., 2007). Analogously in *Nematostella* anthox2 seems to be involved in apical neurogenesis (Galliot and Quiquand, 2011).

Concerning Gsx in protostomes, one of the first works in these organisms is about the polychaete annelid worm, *Capitella teleta*, in which *CapI-Gsx* transcript is transiently expressed during early stages of brain formation, in a subset of anterior neuroectodermal cells (Fröbius and Seaver, 2006). In another annelid worm, the best studied *Platynereis dumerilii*, it was found that the expression of *Pdu-Gsx* is very dynamic. The gene is present, since the pre-larval stage (24hpf), in the prospective neural tissue and later its expression is kept during the differentiation of the trunk CNS. Furthermore, *Pdu-Gsx* is not only restricted to neural regions, being also expressed at larval stage in two bilateral cell clusters in the stomodeum (mouth precursor) and later on in small cell clusters in the midgut and posterior foregut (Hui et al., 2009).

Gsx ortholog in insects is called *ind* and it has been proved that during *Drosophila* embryonic development ind, expressed in the ventral neuroectoderm into two symmetrical columns along the dorsoventral (DV) axis, is one of the key players in patterning DV axis of nervous system (Weiss et al., 1998).

Moving to non-chordate deuterostomes, in *Ambulacraria*, and in particular in the echinoderm *S. purpuratus,* a role of *Gsx* in the developing nervous system can be presumed, given its presence from gastrula through pluteus stages in a small ectodermal domain, probably neural (Arnone et al., 2006).

In *Vertebrates*, after whole genome duplication, two *Gsx* paralogs, named *Gsh1* and *Gsh2* (or *Gsx1* and *Gsx2* too) are present. In *Xenopus tropicalis Gsh1* and *Gsh2* exhibit an expression pattern within the developing nervous system since early neural plate stage and throughout development, in the forebrain, midbrain, hindbrain and spinal cord, with a nice bilaterally symmetrical distribution across the mid-line. In particular, among the territories in which *Gsh1* transcript can be detected, it is worth mentioning pretectum and tectum (two structures involved in processing visual and auditory stimuli), thalamus and hypothalamus, olfactory bulb and a cell population, which gives rise to interneurons. *Gsh2* is more or less expressed in the same territories, even if regions of perfect co-localization with

Gsh1 are quite rare. Of particular relevance is the presence of *Gsh2* also in the endoderm, as occurs in more basal organisms, probably providing a further evidence about the ancestral role of Gsx (Illes *et al.*, 2009).

In mouse, the two genes specifically mark the CNS, with a bilateral distribution similar to the one described for *Xenopus* and Drosophila. Interestingly, Gsh1 is also expressed in the optic stalk (optic nerve primordium. Hsieh-Li et al., 1995; Valerius et al., 1995).

Few expression data are also available for *Gsh1* in medaka fish and zebrafish. In both cases the gene is expressed with a dynamic pattern during development, in many regions of the central nervous system, among which is worth mentioning again hypothalamus primordium, spinal cord (in a region that in zebrafish will generate interneurons) and optic tectum of medaka fish (Deschet et al., 1998; Cheesman and Eisen, 2004).

Given this complex picture, it comes out that Gsx is widely distributed along animal phylogeny, probably exerting its function mainly in the nervous system, through the specification of several cell types and/or the control of their differentiation state. Similarities can be recognized in the width of the expression territories between protostomes (such as annelid and insects) and vertebrates, passing through some cases (echinoderms, urochordates, cephalochordates) in which the gene is restricted in a smaller domain. Based on this observation, one can suppose that the function of Gsx in the Protostome-Deuterostome Ancestor (PDA) was complex and related to a variety of roles in eyes, neurosecretory cells and patterning of the neural tube and then secondarily simplified in the lineages in which it is restricted to smaller patches (Hui et al., 2009).

Obviously, molecular data from as many species as possible are necessary, to outline a clear picture of the functions of this ancient gene during evolution. Our model system *Ciona robusta* exhibits all the required properties to represent a useful joining link for this story.

With regard to *Gsx*, previous studies, done by the former PhD student of my lab, Dr. Rosaria Esposito, revealed a very interesting expression pattern of this gene during *Ciona* development. At

the neural plate stage, *Gsx* is expressed in the a9.33 blastomeres and slightly later it appears also in the a9.37 cells (Fig. 1.11 A, B, C). As development proceeds a further signal appears more posteriorly (green arrow in D, E, F) in a region that is likely to be part of A-lineage descendant, thus indicating that *Gsx* could represent a good marker for the "old" but also for the "revised" photoreceptor cells lineage.

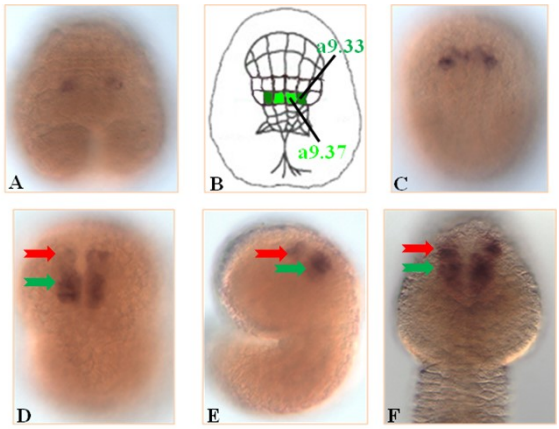

Fig. 1.11 Ci-gsx expression pattern during Ciona robusta development. *WMISH with Ci-gsx probe on embryos at different developmental stages.* ***A.*** *Gastrula, dorsal view.* ***B.*** *Schematic representation of the gastrula stage; a9.33 cell pair is depicted in dark green and a9.37 couple in light green.* ***C.*** *Neurula, dorsal view.* ***D.*** *Middle tailbud, dorsal view.* ***E.*** *Middle tailbud, lateral view.* ***F.*** *Late tailbud, anterior region, dorsal view. In D, E, F: Red arrow indicate the anterior expression, green arrow the posterior expression.*

A further development of my thesis studies thus included a refinement of *Gsx* expression pattern during late *Ciona robusta* development. To this end, I carried out detailed double *in situ* hybridization experiments, using *Gsx* in combination with *FoxB* as marker of A-lineage (A9.14, A9.16 cell pairs), from the neural plate stage, in order to confirm *Gsx* expression also in the "revised" lineage of photoreceptor cell precursors. However, the endogenous *Gsx* gene disappear at the larval stage, so I could not check the localization of *Gsx* in the photoreceptor lineage at the larval stage by double *in situ* hybridization experiments, using *Arrestin* probe as marker for terminal differentiation of these territories. For this aspect of my work, double electroporation experiments, using lineage specific cis-regulatory elements fused to fluorescent reporters, come in handy. In particular I exploited the *pGsx>mCherry* construct, available in the laboratory, in which the 2,8kb *Gsx* cis-regulatory region was fused to *mCherry* reporter gene. *pGsx>mCherry* construct, that is able to recapitulate

endogenous gene expression up the larval stage thanks to the stability of the fluorescent protein product, was used in combination with:

- Arrestin promoter (*pArr*) which labels fully differentiated photoreceptor cells (Yoshida et al., 2004) in the larva.
- Doublesex/mab-3-related promoter (*pDMRT-1*) which labels all the progeny of a-lineage from neural plate to larval stage.
- FoxB promoter (*pFoxB*) which labels all the progeny of A-lineage progeny from neural plate to larval stage.

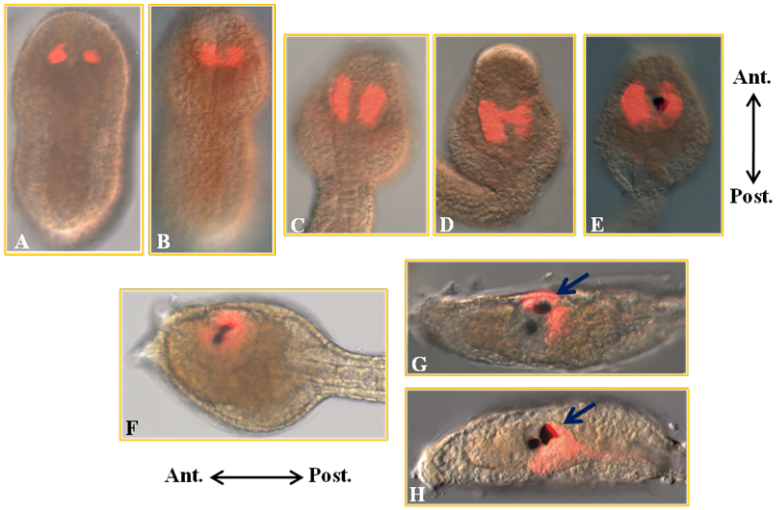

Fig. 1.12 In vivo analysis of pGsx>mCherry construct. *Merged bright-field/fluorescent images are reported. In pictures* ***A-E*** *dorsal view, anterior is on the top;* ***F-H*** *lateral view, anterior is on the left.*
A. *Late neurula stage,* ***B.*** *Middle tailbud stage,* ***C,D****. Late tailbud stages, anterior part of the embryo. Note the different expression of the reporter, due to the mosaic incorporation of the transgene.* ***E.*** *Late tailbud II stage, anterior part of the embryo.* ***F.*** *Late tailbud III stage, anterior part of the embryo, dorso-lateral view.* ***G, H****. Trunk of transgenic larvae; blue arrows indicate the photoreceptor cells region.*

These enhancers were used in different combinations to label specific lineages and visualize them in their final differentiated state in swimming larvae, in order to explore co-localization in larvae of *Gsx*/Arrestin, *Gsx*/a-lineage, *Gsx*/A-lineage, Arrestin/A-lineage, Arrestin/a-lineage.

1.9 Behavioural tests on *Ciona* larvae

During the free-swimming life, *Ciona* larva is exposed to a wide range of environmental stimuli. The

capability to respond in a correct way to environment can make difference between survival and death. Despite the relative simplicity of its CNS, *Ciona* larvae have to perceive and process correctly all external stimuli, in order to be placed at the right place in the right time. In particular in the first part of their life, in the time interval from hatching to 2h post hatching, they start to swim upward to reach surface and this help them to spread. To exert this behaviour, larvae should detect gravity and respond in a negative manner. Slightly later, during free-swimming period, larvae start to display a so-called "light off" response in which they perceive light intensity changes and start to swim faster when brightness decreases. This response starts to be evident since 3h post hatching, because PRCs complete their differentiation and reaches the maximum at 8h post hatching (Kajiwara, 1985). The reason behind this behaviour is to find a suitable substrate, a darker zone underwater, to attach and undergo metamorphosis. As previously mentioned, the swimming behaviour of *Ciona* larvae is under the control of the two pigmented structures present in the sensory vesicle: the ocellus, a light sensing organ, and the otolith, presumably involved in gravity perception (Jiang et al., 2005; Tsuda et al., 2003b). The functions of these organs have been discovered mainly by interfering with the pigmented cells they contain, either through laser ablation, by blocking melanin biosynthesis (Using PTU), or by using mutant lines that specifically disrupt the pigmentation programs. In particular, Tsuda and colleagues (Tsuda et al., 2003b) have been the first to demonstrate that the anterior pigment cell (otolith) is linked to the upward swimming behaviour, while the posterior pigment cell (ocellus) is responsible for the photo-responsive component of swimming behaviour. Furthermore, their studies suggested that the swimming behaviour of *Ciona* larvae is not affected by the pressure, and this represents the only study on this topic in *Ciona*.

1.9.1 Third aim of the thesis

In the attempt to better and deeper explore if the behaviour of *Ciona* larvae is influenced by changes of pressure in the surrounding environment, I spent last months of my Phd in the Laboratory head by

Dr. Gáspar Jékely, at the Max Planck Institute for developmental biology. There, in collaboration with Dr. Luis Bezares, my studies were devoted to 1) a detailed investigation of the behavior of free-swimming larvae exposed to different pressure levels and to 2) the identification of *Ciona* larval structure involved in the detection of hydrostatic pressure.

Hydrostatic pressure is the force per unit area exerted by a liquid on an object. Hydrostatic pressure increases in proportion to depth (1 bar each 10 meters) measured from the surface, due to the increasing weight of the fluid that exerts downward force. In addition, if the liquid is in contact with a gas, the total pressure is the sum of the pressure of the gas plus the pressure of the liquid (Ptotal = Patmosphere + Pfluid).

To detect and characterize the behavior of larvae exposed to increased pressure levels, I used the chamber designed by Dr. Bezares and the recording setup available in the hosting laboratory. At the same time, I devoted my attention on the dopamine (DA)-synthesizing putative sensory neurons, the so-called coronet cells (Fig. 1.7), present in the sensory vesicle (Eakin and Kuda, 1971; Moret et al., 2005a; Nicol and Meinertzhagen, 1991) as potential organs involved in pressure detection. To this end, I prepared the construct pTH/GCaMP in which the TH (tyrosine hydroxylase) promoter, available in the Laboratory, which specifically labels dopamine cells (Moret et al., 2005b), was cloned upstream of the GCaMP (genetically encoded calcium indicator), a reporter that represents a powerful tool to identify activated neurons, by monitoring calcium influx (see Material and methods). This construct was electroporated in *Ciona* fertilized eggs and the resulting larvae were then subjected to an in-vivo imaging scan, under the confocal microscope, in a particular holding chamber in which it was possible to increase the pressure during the observation.

Bibliography

Abitua, P.B., Gainous, T.B., Kaczmarczyk, A.N., Winchell, C.J., Hudson, C., Kamata, K., Nakagawa, M., Tsuda, M., Kusakabe, T.G., Levine, M., 2015. The pre-vertebrate origins of neurogenic placodes. Nature 524, 462-465.

Alfano, C., Teresa Russo, M., Spagnuolo, A., 2007. Developmental expression and transcriptional regulation of Ci-Pans, a novel neural marker gene of the ascidian, Ciona intestinalis. Gene 406, 36-41.

Arnone MI, Rizzo F, Annunziata R, Cameron RA, Peterson KJ, Martinez P. (2006). Genetic organization and embryonic expression of the ParaHox genes in the sea urchin S. purpuratus: insights into the relationship between clustering and colinearity. Dev Biol, 300: 63-73.

Aros, B., Viragh, S., 1969. Fine structure of the pharynx and endostyle of an ascidian (Ciona intestinalis). Acta Biol Acad Sci Hung 20, 281-297.

Arshavsky, V. Y., 2002. Rhodopsin phosphorylation: from terminating single photon responses to photoreceptor dark adaptation. Trends Neurosci. 25, 124-6.

Bailey TJ, El-Hodiri H, Zhang L, Shah R, Mathers PH, Jamrich M. (2004). Regulation of vertebrate eye development by Rx genes. Int J Dev Biol, 48: 761-70.

Beaster-Jones, L., Kaltenbach, S.L., Koop, D., Yuan, S., Chastain, R., Holland, L.Z., 2008. Expression of somite segmentation genes in amphioxus: a clock without a wavefront? Dev Genes Evol 218, 599-611.

Bertrand, V., Hudson, C., Caillol, D., Popovici, C., Lemaire, P., 2003. Neural tissue in ascidian embryos is induced by FGF9/16/20, acting via a combination of maternal GATA and Ets transcription factors. Cell 115, 615-627.

Blomhoff, R., Blomhoff, H. K., 2006. Overview of retinoid metabolism and function. J Neurobiol. 66, 606-30.

Bray, S. J. (2006). "Notch signalling: a simple pathway becomes complex." Nat Rev Mol Cell Biol 7(9): 678-689.

Brooke, N. M., Garcia-Fernandez, J., Holland, P. W., 1998. The ParaHox gene cluster is an evolutionary sister of the Hox gene cluster. Nature. 392, 920-2.

Brunetti, R.G., C.; Pennati, R.; Caicci, F.; Gasparini, F.; Manni, L., 2015. Morphological evidence that the molecularly determined Ciona intestinalis type A and type B are different species: Ciona robusta and Ciona intestinalis. journal of zoological systematics and evolutionary research 53, 186-193.

Brusca, R.C., Brusca, G.J. , 2003. The urochodates (tunicates), in Invertebrates. 2nd edn, Sinauer Assoc. Inc, Sunderland, MA,, 855-886.

Callaerts P, Halder G. Gehring WJ. (1997). PAX-6 in development and evolution. Annu Rev Neurosci, 20: 483-532.

Capellini, T.D., Dunn, M.P., Passamaneck, Y.J., Selleri, L., Di Gregorio, A., 2008. Conservation of notochord gene expression across chordates: insights from the Leprecan gene family. Genesis 46, 683-696.

Caracciolo A, Gesualdo I, Branno M, Aniello F, Di Lauro R, Palumbo A. (1997). Specific cellular localization of tyrosinase mRNA during Ciona intestinalis larval development. Dev Growth Differ, 39: 437-44.

Chabry, L., 1887. Contribution to the normal and teratological embryology of solitary ascidians

Cheesman SE and Eisen JS. (2004). gsh1 demarcates hypothalamus and intermediate spinal cord in zebrafish. Gene Expr Patterns, 5:107-12.

Christiaen, L., Jaszczyszyn, Y., Kerfant, M., Kano, S., Thermes, V., Joly, J.S., 2007.

Christiaen, L., Wagner, E., Shi, W., Levine, M., 2009. Electroporation of transgenic DNAs in the sea squirt Ciona. Cold Spring Harb Protoc 2009, pdb prot5345.

Cole, A.G., Meinertzhagen, I.A., 2004. The central nervous system of the ascidian larva: mitotic history of cells forming the neural tube in late embryonic Ciona intestinalis. Dev Biol 271, 239-262.

Conklin, E.G., 1905. The organization and cell lineage of the ascidian egg. J Acad Natl Sci (Philadelphia) 13, 1–119.

Corbo, J.C., Levine, M., Zeller, R.W., 1997. Characterization of a notochord-specific enhancer from the Brachyury promoter region of the ascidian, Ciona intestinalis. Development 124, 589-602.

Crowther, R.J., Whittaker, J.R., 1992. Structure of the caudal neural tube in an ascidian larva: vestiges of its possible evolutionary origin from a ciliated band. J Neurobiol 23, 280-292.

D'Aniello S, D'Aniello E, Locascio A, Memoli A, Corrado M, Russo MT, Aniello F, Fucci L, Brown ER, Branno M. (2006). The ascidian homolog of the vertebrate homeobox gene Rx is essential for ocellus development and function. Differentiation, 74: 222-34.

Dehal, P., Satou, Y., Campbell, R.K., Chapman, J., Degnan, B., De Tomaso, A., Davidson, B., Di Gregorio, A., Gelpke, M., Goodstein, D.M., Harafuji, N., Hastings, K.E., Ho, I., Hotta, K., Huang, W., Kawashima, T., Lemaire, P., Martinez, D., Meinertzhagen, I.A., Necula, S., Nonaka, M., Putnam, N., Rash, S., Saiga, H., Satake, M., Terry, A., Yamada, L., Wang, H.G., Awazu, S., Azumi, K., Boore, J., Branno, M., Chin-Bow, S., DeSantis, R., Doyle, S., Francino, P., Keys, D.N., Haga, S., Hayashi, H., Hino, K., Imai, K.S., Inaba, K., Kano, S., Kobayashi, K., Kobayashi, M., Lee, B.I., Makabe, K.W., Manohar, C., Matassi, G., Medina, M., Mochizuki, Y., Mount, S., Morishita, T., Miura, S., Nakayama, A., Nishizaka, S., Nomoto, H., Ohta, F., Oishi, K., Rigoutsos, I., Sano, M., Sasaki, A., Sasakura, Y., Shoguchi, E., Shin-i, T., Spagnuolo, A., Stainier, D., Suzuki, M.M., Tassy, O., Takatori, N., Tokuoka, M., Yagi, K., Yoshizaki, F., Wada, S., Zhang, C., Hyatt, P.D., Larimer, F., Detter, C., Doggett, N., Glavina, T., Hawkins, T., Richardson, P., Lucas, S., Kohara, Y., Levine, M., Satoh, N., Rokhsar, D.S., 2002. The draft genome of Ciona intestinalis: insights into chordate and vertebrate origins. Science 298, 2157-2167.

del Marmol V and Beermann F. (1996). Tyrosinase and related proteins in mammalian pigmentation. FEBS Lett, 381: 165-8.

Delsuc, F., Brinkmann, H., Chourrout, D., Philippe, H., 2006. Tunicates and not cephalochordates are the closest living relatives of vertebrates. Nature 439, 965-968.

Deschet K, Bourrat F, Chourrout D, Joly JS. (1998). Expression domains of the medaka (Oryzias latipes) Ol-Gsh 1 gene are reminiscent of those of clustered and orphan homeobox genes. Dev Genes Evol, 208: 235-44.

Dufour, H.D., Chettouh, Z., Deyts, C., de Rosa, R., Goridis, C., Joly, J.S., Brunet, J.F., 2006. Precraniate origin of cranial motoneurons. Proc Natl Acad Sci U S A 103, 8727-8732.

Eakin, R.M., Kuda, A., 1971. Ultrastructure of sensory receptors in Ascidian tadpoles. Z Zellforsch Mikrosk Anat 112, 287-312.

Eales, J.G., 1997. Iodine metabolism and thyroid-related functions in organisms lacking thyroid follicles: are thyroid hormones also vitamins? Proc Soc Exp Biol Med 214, 302-317.

Esposito R, D'Aniello S, Squarzoni P, Pezzotti MR, Ristoratore F, Spagnuolo A. (2012). New insights into the evolution of metazoan tyrosinase gene family. PLoS ONE, 7(4): e35731. Evolutionary modification of mouth position in deuterostomes. Semin Cell Dev Biol 18, 502-511.

Fanelli, A., Lania, G., Spagnuolo, A., Di Lauro, R., 2003. Interplay of negative and positive signals controls endoderm-specific expression of the ascidian Cititf1 gene promoter. Dev Biol 263, 12-23.

Finnerty JR, Paulson D, Burton P, Pang K, Martindale MQ. (2003). Early evolution of a homeobox gene: the parahox gene Gsx in the Cnidaria and the Bilateria. Evol Dev, 5: 331-45.

Fröbius AC and Seaver EC. (2006). ParaHox gene expression in the polychaetes annelid Capitella sp I. Dev Genes Evol, 216: 81-8.

Gainous, T.B., Wagner, E., Levine, M., 2015. Diverse ETS transcription factors mediate FGF signaling in the Ciona anterior neural plate. Dev Biol 399, 218-225.

Galliot B and Quiquand M. (2011). A two-step process in the emergence of neurogenesis. Eur J Neurosci, 34: 847-62.

Germain, S., Howell, M., Esslemont, G.M., Hill, C.S., 2000. Homeodomain and winged-helix transcription factors recruit activated Smads to distinct promoter elements via a common Smad interaction motif. Genes Dev 14, 435-451.

Glardon S, Callaerts P, Halder G, Gehring WJ. (1997). Conservation of Pax-6 in a lower chordate, the ascidian Phallusia mammillata. Development, 124: 817-25.

Gorman, A. L., McReynolds, J. S., Barnes, S. N., 1971. Photoreceptors in primitive chordates: fine structure, hyperpolarizing receptor potentials, and evolution. Science. 172, 1052-4.

Halder G, Callaerts P, Gehring WJ. (1995). Induction of ectopic eyes by targeted expression of the eyeless gene in Drosophila. Science, 267: 1788-92.

Haupaix, N., Abitua, P.B., Sirour, C., Yasuo, H., Levine, M., Hudson, C., 2014. Ephrin-mediated restriction of ERK1/2 activity delimits the number of pigment cells in the Ciona CNS. Dev Biol 394, 170-180.

Horie, T., Kusakabe, T., Tsuda, M., 2008a. Glutamatergic networks in the Ciona intestinalis larva. J Comp Neurol 508, 249-263.

Horie, T., Orii, H., Nakagawa, M., 2005. Structure of ocellus photoreceptors in the ascidian Ciona intestinalis larva as revealed by an anti-arrestin antibody. J Neurobiol 65, 241-250.

Horie, T., Sakurai, D., Ohtsuki, H., Terakita, A., Shichida, Y., Usukura, J., Kusakabe, T., Tsuda, M., 2008b. Pigmented and nonpigmented ocelli in the brain vesicle of the ascidian larva. J Comp Neurol 509, 88-102.

Hsieh-Li HM, Witte DP, Szucsik JC, Weinstein M, Li H, Potter SS. (1995). Gsh-2, a murine homeobox gene expressed in the developing brain. Mech Dev, 50: 177-86.

Hudson, C., Lotito, S., Yasuo, H., 2007. Sequential and combinatorial inputs from Nodal, Delta2/Notch and FGF/MEK/ERK signalling pathways establish a grid-like organisation of distinct cell identities in the ascidian neural plate. Development 134, 3527-3537.

Hudson, C., Sirour, C., Yasuo, H., 2015. Snail mediates medial-lateral patterning of the ascidian neural plate. Dev Biol 403, 172-179.

Hudson, C., Yasuo, H., 2005. Patterning across the ascidian neural plate by lateral Nodal signalling sources. Development 132, 1199-1210.

Hui JH, Raible F, Korchagina N, Dray N, Samain S, Magdelenat G, Jubin C, Segurens B, Balavoine G, Arendt D, Ferrier DE. (2009). Features of the ancestral bilaterian inferred from Platynereis dumerilii ParaHox genes. BMC Biol, 7: 43.

Illes JC, Winterbottom E, Isaacs, HV. (2009). Cloning and expressionvanalysis of the anterior parahox genes, Gsh1 and Gsh2 from Xenopus tropicalis. Dev Dyn, 238: 194-203.

Imai, J.H., Meinertzhagen, I.A., 2007. Neurons of the ascidian larval nervous system in Ciona intestinalis: I. Central nervous system. J Comp Neurol 501, 316-334.

Imai, K.S., Levine, M., Satoh, N., Satou, Y., 2006. Regulatory blueprint for a chordate embryo. Science 312, 1183-1187.

Jiang, D., Tresser, J.W., Horie, T., Tsuda, M., Smith, W.C., 2005. Pigmentation in the sensory organs of the ascidian larva is essential for normal behavior. J Exp Biol 208, 433-438.

Johnson, D.S., Davidson, B., Brown, C.D., Smith, W.C., Sidow, A., 2004. Noncoding regulatory sequences of Ciona exhibit strong correspondence between evolutionary constraint and functional importance. Genome Res 14, 2448-2456.

Kajiwara, S.Y., M., 1985. Change in behaviour and ocellar structure during the larval life of solitary ascidians. Biol Bull. 169, 565-577.

Kusakabe, T., Kusakabe, R., Kawakami, I., Satou, Y., Satoh, N., Tsuda, M., 2001. Ci-opsin1, a vertebrate-type opsin gene, expressed in the larval ocellus of the ascidian Ciona intestinalis. FEBS Lett. 506, 69-72.

Lamb, T. D., Collin, S. P., Pugh, E. N., Jr., 2007. Evolution of the vertebrate eye: opsins, photoreceptors, retina and eye cup. Nat Rev Neurosci. 8, 960-76.

Lemaire, P., Bertrand, V., Hudson, C., 2002. Early steps in the formation of neural tissue in ascidian embryos. Dev Biol 252, 151-169.

Lewin B. (2000). Homeodomains bind related targets in DNA. In Genes VII. Oxford: Oxford University Pres, 660-2.

Linnè, 1767. Systema naturae per regna tria naturae: secundum classes, ordines, genera, species, cum characteribus, differentiis, synonymis, locis,Uppsala.

Marikawa, Y., Yoshida, S., Satoh, N., 1994. Development of egg fragments of the ascidian Ciona savignyi: the cytoplasmic factors responsible for muscle differentiation are separated into a specific fragment. Dev Biol 162, 134-142.

Mazet F, Hutt JA, Millard J, Shimeld SM. (2003). Pax gene expression in the developing central nervous system of Ciona intestinalis. Gene Expr Patterns, 3: 743-5.

McGinnis W, Levine MS, Hafen E, Kuroiwa A, Gehring WJ. (1984). A conserved DNA sequence in homoeotic genes of the Drosophila Antennapedia and bithorax complexes. Nature, 308: 428-33.

Meinertzhagen, I.A., Lemaire, P., Okamura, Y., 2004. The neurobiology of the ascidian tadpole larva: recent developments in an ancient chordate. Annu Rev Neurosci 27, 453-485.

Meinertzhagen, I.A., Okamura, Y., 2001. The larval ascidian nervous system: the chordate brain from its small beginnings. Trends Neurosci 24, 401-410.

Miljkovic-Licina M, Chera S, Ghila L, Galliot B. (2007). Head regeneration in wild-type hydra requires de novo neurogenesis. Development, 134: 1191-201.

MJ., K., 1983. Comparative anatomy of the tunicate tadpole, Ciona intestinalis. Biol Bull. 164, 1-27.

Moret, F., Christiaen, L., Deyts, C., Blin, M., Joly, J.S., Vernier, P., 2005a. The dopamine-synthesizing cells in the swimming larva of the tunicate Ciona intestinalis are located only in the hypothalamus-related domain of the sensory vesicle. Eur J Neurosci 21, 3043-3055.

Moret, F., Christiaen, L., Deyts, C., Blin, M., Vernier, P., Joly, J.S., 2005b. Regulatory gene expressions in the ascidian ventral sensory vesicle: evolutionary relationships with the vertebrate hypothalamus. Dev Biol 277, 567-579.

Morgan, T., 1923. Removal of the block to self-fertilization in the ascidians Ciona. Proc Natl Acad Sci U S A 9, 170.

Nakagawa, M., Orii, H., Yoshida, N., Jojima, E., Horie, T., Yoshida, R., Haga, T., Tsuda, M., 2002. Ascidian arrestin (Ci-arr), the origin of the visual and nonvisual arrestins of vertebrate. Eur J Biochem. 269, 5112-8.

Nakashima, K., Yamada, L., Satou, Y., Azuma, J., Satoh, N., 2004. The evolutionary origin of animal cellulose synthase. Dev Genes Evol. 214, 81-8.

Nicol, D., Meinertzhagen, I.A., 1991. Cell counts and maps in the larval central nervous system of the ascidian Ciona intestinalis (L.). J Comp Neurol 309, 415-429.

Nishida, H., 1987. Cell lineage analysis in ascidian embryos by intracellular injection of a tracer enzyme. III. Up to the tissue restricted stage. Dev Biol 121, 526-541.

Ohtsuka, Y., Matsumoto, J., Katsuyama, Y., Okamura, Y., 2014. Nodal signaling regulates specification of ascidian peripheral neurons through control of the BMP signal. Development 141, 3889-3899.

Okada, T., Hirano, H., Takahashi, K., Okamura, Y., 1997. Distinct neuronal lineages of the ascidian embryo revealed by expression of a sodium channel gene. Dev Biol 190, 257-272.

Okada, T., Katsuyama, Y., Ono, F., Okamura, Y., 2002. The development of three identified motor neurons in the larva of an ascidian, Halocynthia roretzi. Dev Biol 244, 278-292.

Ortolani, G. (1964). "[the Fate of the A7.6 Cells in Ascidian Eggs]." Ric Sci 2 Ser Pt 2 Rend B 47: 525-526.

PN., D., 1969. Studies on the receptors in Ciona intestinalis. 3. A second type of photoreceptor in the tadpole larva of Ciona intestinali. Z Zellforsch Mikrosk Anat 96, 63-65.

Putnam, N.H., Butts, T., Ferrier, D.E., Furlong, R.F., Hellsten, U., Kawashima, T., Robinson-Rechavi, M., Shoguchi, E., Terry, A., Yu, J.K., Benito-Gutierrez, E.L., Dubchak, I., Garcia-Fernandez, J., Gibson-Brown, J.J., Grigoriev, I.V., Horton, A.C., de Jong, P.J., Jurka, J., Kapitonov, V.V., Kohara, Y., Kuroki, Y., Lindquist, E., Lucas, S., Osoegawa, K., Pennacchio, L.A., Salamov, A.A., Satou, Y., Sauka-Spengler, T., Schmutz, J., Shin, I.T., Toyoda, A., Bronner-Fraser, M., Fujiyama, A., Holland, L.Z., Holland, P.W., Satoh, N., Rokhsar, D.S., 2008. The amphioxus genome and the evolution of the chordate karyotype. Nature 453, 1064-1071.

Q., B., 1992. On the locomotion of ascidian tadpole larvae. j.mar.biol 72, 161-186.

Racioppi, C., Kamal, A.K., Razy-Krajka, F., Gambardella, G., Zanetti, L., di Bernardo, D., Sanges, R., Christiaen, L.A., Ristoratore, F., 2014. Fibroblast growth factor signalling controls nervous system patterning and pigment cell formation in Ciona intestinalis. Nat Commun 5, 4830.

Randall, R.A., Howell, M., Page, C.S., Daly, A., Bates, P.A., Hill, C.S., 2004. Recognition of phosphorylated-Smad2-containing complexes by a novel Smad interaction motif. Mol Cell Biol 24, 1106-1121.

Razy-Krajka, F., Brown, E.R., Horie, T., Callebert, J., Sasakura, Y., Joly, J.S., Kusakabe, T.G., Vernier, P., 2012. Monoaminergic modulation of photoreception in ascidian: evidence for a proto-hypothalamo-retinal territory. BMC Biol 10, 45.

Ryan, K., Lu, Z., Meinertzhagen, I.A., 2016. The CNS connectome of a tadpole larva of Ciona intestinalis (L.) highlights sidedness in the brain of a chordate sibling. Elife 5.

Sakurai, D., Goda, M., Kohmura, Y., Horie, T., Iwamoto, H., Ohtsuki, H., Tsuda, M., 2004. The role of pigment cells in the brain of ascidian larva. J Comp Neurol 475, 70-82.

Sasaki, H., Yoshida, K., Hozumi, A., Sasakura, Y., 2014. CRISPR/Cas9-mediated gene knockout in the ascidian Ciona intestinalis. Dev Growth Differ 56, 499-510.

Sato S , Masuya H, Numakunai T, Satoh N, Ikeo K, Gojobori T, Tamura K, Ide H, Takeuchi T, Yamamoto H. (1997). Ascidian tyrosinase gene: its unique structure and expression in the developing brain. Dev Dyn, 208: 363-74.

Sato, S., Yamamoto, H., 2001. Development of pigment cells in the brain of ascidian tadpole larvae: insights into the origins of vertebrate pigment cells. . Pigment Cell Res. 14, 428-36.

Satoh, N., 2001. Ascidian embryos as a model system to analyze expression and function of developmental genes. Differentiation 68, 1-12.

Satoh, N., 2003. The ascidian tadpole larva: comparative molecular development and genomics. Nat Rev Genet 4, 285-295.

Satoh, N., 2014. Developmental Genomics of Ascidians, First Edition.

Satou, Y., Satoh, N., 2005. Cataloging transcription factor and major signaling molecule genes for functional genomic studies in Ciona intestinalis. Dev Genes Evol 215, 580-596.

Satou, Y., Yamada, L., Mochizuki, Y., Takatori, N., Kawashima, T., Sasaki, A., Hamaguchi, M., Awazu, S., Yagi, K., Sasakura, Y., Nakayama, A., Ishikawa, H., Inaba, K., Satoh, N., 2002. A cDNA resource from the basal chordate Ciona intestinalis. Genesis 33, 153-154.

Schubert, M., Escriva, H., Xavier-Neto, J., Laudet, V., 2006. Amphioxus and tunicates as evolutionary model systems. Trends Ecol Evol 21, 269-277.

Scott MP and Weiner AJ. (1984). Structural relationships among genes that control development: sequence homology between the Antennapedia, Ultrabithorax, and fushi tarazu loci of Drosophila. Proc Natl Acad Sci USA, 81: 4115-9.

Squarzoni, P., Parveen, F., Zanetti, L., Ristoratore, F., Spagnuolo, A., 2011. FGF/MAPK/Ets signaling renders pigment cell precursors competent to respond to Wnt signal by directly controlling Ci-Tcf transcription. Development 138, 1421-1432.

Stolfi, A., Gandhi, S., Salek, F., Christiaen, L., 2014. Tissue-specific genome editing in Ciona embryos by CRISPR/Cas9. Development 141, 4115-4120.

Svane, I., Young, C. M. , 1989 The ecology and behaviour of ascidian larvae. Oceanogr. mar. Biol. A. Rev. 27, 45-90.

Szebenyi, G. and J. F. Fallon (1999). "Fibroblast growth factors as multifunctional signaling factors." Int Rev Cytol 185: 45-106.

Takahashi, H., Mitani, Y., Satoh, G., Satoh, N., 1999. Evolutionary alterations of the minimal promoter for notochord-specific Brachyury expression in ascidian embryos. Development 126, 3725-3734.

Takimoto N, Kusakabe T, Horie T, Miyamoto Y, Tsuda M. (2006). Origin of the vertebrate visual cycle: III. Distinct distribution of RPE65 and beta-carotene 15,15'-monooxygenase homologues in Ciona intestinalis. Photochem Photobiol, 82: 1468-74.

Treen, N., Yoshida, K., Sakuma, T., Sasaki, H., Kawai, N., Yamamoto, T., Sasakura, Y., 2014. Tissue-specific and ubiquitous gene knockouts by TALEN electroporation provide new approaches to investigating gene function in Ciona. Development 141, 481-487.

Treisman J, Gönczy P, Vashishtha M, Harris E, Desplan C. (1989). A single amino acid can determine the DNA binding specificity of homeodomain proteins. Cell, 59: 553-62.

Treisman J, Harris E, Wilson D, Desplan C. (1992). The homeodomain: a new face for the helix-turn-helix? Bioessays 14: 145-50.

Tsuda, M., Sakurai, D., Goda, M., 2003b. Direct evidence for the role of pigment cells in the brain of ascidian larvae by laser ablation. J Exp Biol 206, 1409-1417.

Valerius MT, Li H, Stock JL, Weinstein M, Kaur S, Singh G, Potter SS. (1995). Gsh-1: a novel murine homeobox gene expressed in the central nervous system. Dev Dyn, 203: 337-51.

Vienne, A., Pontarotti, P., 2006. Metaphylogeny of 82 gene families sheds a new light on chordate evolution. Int J Biol Sci 2, 32-37.

Wada, S. and H. Saiga (1999). "Cloning and embryonic expression of Hrsna, a snail family gene of the ascidian Halocynthia roretzi: implication in the origins of mechanisms for mesoderm specification and body axis formation in chordates." Dev Growth Differ **41**(1): 9-18.

Wasylyk, B., Hagman, J., Gutierrez-Hartmann, A., 1998. Ets transcription factors: nuclear effectors of the Ras-MAP-kinase signaling pathway. Trends Biochem Sci 23, 213-216.

Weiss JB, Von Ohlen T, Mellerick D, Dressler G, Doe CQ, Scott MP. (1998). Dorsoventral patterning in the Drosophila Central Nervous System: the intermediate neuroblasts defective Homeobox gene specifies intermediate column identity. Genes Dev, 12: 3591-602.

Whittaker, J.R., 1977. Segregation during cleavage of a factor determining endodermal alkaline phosphatase development in ascidian embryos. J Exp Zool 202, 139-153.

Yoshida, R., Sakurai, D., Horie, T., Kawakami, I., Tsuda, M., Kusakabe, T., 2004. Identification of neuron-specific promoters in Ciona intestinalis. Genesis 39, 130-140.

Chapter 2

Materials and Methods

Materials and Methods

2.1 *Ciona robusta* eggs and embryos collection

Ciona robusta adults were collected in the bay of Naples or Taranto, and maintained at the Aquaculture Service of Stazione Zoologica A. Dohrn (Naples) under constant illumination, in sea water tanks equipped with appropriate water circulation and filtering system. Ripe oocytes and sperm were collected surgically and kept separately until in vitro fertilization. Fertilized eggs were used for behavioral test, transgenesis, drug treatment, and *in situ* hybridization experiments. Embryos were raised in Millipore-filtered sea water (MFSW) at 18-20°C.

2.2 Wild-type embryos for behavioral tests

To perform behavioral tests wild-type embryos were generated by *in vitro* fertilization. Oocytes and sperm were collected surgically from at least two different animals. The gametes were incubated for 10 minutes in a Petri dish coated with 1% agarose to perform an *in vitro* fertilization in MFSW. After 10 minutes fertilized eggs were washed several time and transferred in a bigger Petri dish of 10 cm of diameter with a thin layer of 1% agarose. The animals have been grown in MFSW at 18°C.

2.3 Chemical dechorionation and *in vitro* fertilization

Before to perform electroporation of the fertilized eggs, it is necessary to deprive the eggs of the chorion. The chemical dechorionation has been effectuated in a glass tube in MFSW, putting the eggs for 5-6 minutes in a pH 10 solution of Thioglycolic acid (1%) and Proteinase E (0.05%) in MFSW. During this time, the eggs have been shaken continuously in this solution, using a glass pipette, to remove the chorion and the follicular cells surrounding the eggs. After this step the eggs have been washed several times to remove the residual solution and then fertilized *in vitro,* in a small Petri dish coated with a thin layer of 1% agarose, with sperm collected from two or more individuals to avoid self-sterility problems. After 10 minutes, fertilized eggs have been washed 2-4 times to eliminate the

exceeding sperm and then have been used for transgenesis experiments. Alternatively, the embryos have been grown in MFSW at 18-20°C, and fixed at the suitable stages to perform whole-mount *in situ* hybridization (WMISH) or fixed for reporter signal analysis.

2.4 Transgenesis *via* electroporation

The fertilized eggs have been immediately transferred in a solution containing 0.77 M Mannitol and 50-100 μg of DNA. The electroporation has been carried out in Bio-Rad Gene Pulser 0.4 cm cuvettes, using a Bio-Rad Gene Pulser II electroporator, at constant 50 V and 500-800 μF, in order to have a time constant of 14-20 m/seconds. The embryos have been allowed to develop until the desired stage on 1% agarose coated Petri dishes, at 18-20°C. Depending on the electroporated constructs and on the purposes of the experiment, the embryos have been fixed for Whole Mount *in situ* Hybridization or analyzed at the microscope.

In order to be sure of the electroporation success, only the experiments in which at least 60% of the embryos developed normally were selected for analyses. All the constructs have been tested in at least three different batch of animals; percentages reported in the results have been calculated taking in to consideration at least 100 embryos for each construct.

2.5 Embryos observation and imaging analyses

For the observation at the microscope of fluorescence and phenotypes, embryos and larvae have been observed *in vivo*. To avoid embryos movement, late tailbud and larvae have been sedated using menthol crystals in the sea water. The embryos have been then placed on a microscope slide; a cover slide with some plasticine at the corners have been positioned on the top of a sea water drop, containing the embryos, and pressed until the volume resulted uniformly distributed. DIC and fluorescent images have been taken with a Zeiss Axio Imager M1 microscope equipped with an Axiocam digital camera.

For confocal images, embryos have been analyzed with a Zeiss confocal laser scanning microscope LSM 510 and more recently with a Leica SP8-x.

2.6 PCR amplification from genomic or plasmid DNA

The PCR reactions have been performed in a total volume of 50 µl, using about 100 ng of DNA as template, 0.2 mM of dNTP mix (dATP, dTTP, dCTP, dGTP), 1x PCR buffer (Roche), 0.05U/µl of Taq DNA polymerase (Roche) and 2 pmol/µl of each forward and reverse suitable oligonucleotides. The PCR amplification program has been set as follows.

- First step (1 cycle). DNA denaturation: 5' at 95°C.
- Second step (repeated for 35 cycles).

  DNA denaturation: 1' at 95°C.

  Oligonucleotides annealing: 2' at the suitable temperature for plasmid DNA, 4' at suitable temperature for genomic DNA (the temperature used in this step has been set at least 5-8°C below the melting temperature of the oligonucleotides).

  Polymerization: 72°C for a suitable time, calculated considering the desired amplified fragment length and the Taq DNA Polymerase processivity, that is around 1 Kb/minute.
- Final elongation step: 10' at 72°C.

The amplified fragments have been separated from the template DNA and from dNTPs and oligonucleotide excess by gel electrophoresis using, as fragment length marker, 1x GeneRuler™ 1Kb DNA Ladder (Fermentas), 1x GeneRuler™ 100 bp DNA Ladder (Fermentas) or 1x Lambda DNA/HindIII, 2 (Fermentas), according to the expected length of the fragment.

The fragments have been isolated and purified by gel extraction (GenElute™Gel Extraction Kit, Sigma). The concentration have been evaluated by gel electrophoresis using as marker 1x Lambda DNA/HindIII, 2 (Fermentas).

2.7 DNA gel electrophoresis

Preparative and analytic DNA gel electrophoreses have been performed on 0.8%, 1% or 1.5% of agarose gel in 1x TAE buffer (Stock solution 50x: 252 g of Tris base; 57.1 ml glacial acetic acid; 100 ml 0.5 M EDTA; H_20 to 1 liter), considering the length of the DNA to be run and adding 0.5 μg/ml Ethidium Bromide (EtBr).

2.8 DNA gel extraction

Digested and PCR amplified fragments have been extracted from gel cutting them with a sterile sharpen blade, using the GenElute™ Gel Extraction Kit (Sigma-Aldrich), following the manufacturer's instructions. After the extraction, the concentration has been estimated by gel electrophoresis.

2.9 DNA digestions with restriction endonucleases

Analytic and preparative plasmid DNA digestions have been performed with the appropriate restriction endonucleases in total volumes of at least 20 times more than the enzyme volume used. The digestion reaction has been prepared as follows: the solution contained the desired amount of DNA, suitable restriction enzyme buffer (1/10 Roche; New England Biolabs; Amersham), restriction enzyme/s (5 units enzyme per 1 μg of DNA) and BSA (1/100, if required). Reaction specific temperatures have been used as suggested by manufacturer's instructions.

2.10 DNA dephosphorylation

In order to prevent self-ligation, a convenient amount of double strand linearized DNA has been incubated with 1U of Calf Intestinalis Alkaline Phosphatase enzyme (CIAP; Roche) per 1 pmol 5' ends of linearized DNA, in 1x CIP dephosphorylation buffer (Roche), at 37°C for 30'. After this time, a second aliquot of CIAP has been added, and the reaction has been carried on for another 30', at 37°C. Subsequently, the dephosphorylated DNA has been purified by gel extraction.

2.11 DNA ligation

Each ligation reaction has been carried out in a final volume of 20 µl mixture containing 1x T4 Ligase buffer (50 mM Tris-HCl pH 7.5, 10 mM $MgCl_2$, 10 mM dithiothreitol, 1 mM ATP, pH 7.5) and 1 µl of T4 DNA Ligase (New England Biolabs) at 1U/ µl. The proportion of plasmid vector and insert DNA was usually kept 1:4, and the total amount of DNA was kept within 50-100 ng. The reaction mix has been incubated at 16 °C overnight or 1,5 hour at R.T., and used to transform competent bacteria.

2.12 Bacterial cells electroporation

By this approach it is possible to transform bacterial cells with plasmids containing DNA of interest. Briefly, the circular plasmid DNA and competent *E. coli* bacterial cells (prepared by the Molecular Biology Service of the Stazione Zoologica A. Dohrn in Naples), were placed in a 0.2 cm electrocuvette. The electrocuvette was subjected to an electric pulse at constant 1.7 V using a Bio-Rad Gene Pulser™ electroporation apparatus.

The transformed *E. coli* cells were allowed to recover for one hour at 37ºC in 1ml LB medium (NaCl 10g/l, bactotryptone 10g/l, yeast extract 5g/l,). An aliquot was spread on a pre-warmed LB solid medium (NaCl 10g/l, bactotryptone 10g/l, yeast extract 5g/l, agar 15g/l) in the presence of specific selective antibiotic and grown at the same temperature overnight.

2.13 PCR screening

It is possible to carry out a PCR reaction using as template a single bacterial colony and in the same time grow the colony. Half of each single colony was placed in a PCR mixture described below, and half grown in 3 ml of LB liquid medium in the presence of the suitable antibiotic (50µg/ml), 8-12 hours shaking at 270 rpm, at 37 ºC.

The PCR reactions have been set in a total volume of 20 µl, with the following composition: 1x PCR buffer (Roche); 0.2 mM dNTP mix (dATP, dTTP, dCTP, dGTP); 1 pmol/µl of each forward and

reverse suitable oligonucleotides; and 0.025 U/µl Taq DNA polymerase (Roche; Biogem). PCRs have been carried out with the following protocol:

- First step (1 cycle). DNA denaturation: 5' at 95°C.
- Second step (repeated for 30 cycles).

  DNA denaturation: 1' at 94°C.

  Oligonucleotides annealing: 1' at the suitable temperature (according to the melting temperature of oligonucleotides)

  Polymerization: 72°C for a suitable time (1 min/kb).

By gel electrophoresis analysis, the samples presenting a band of expected sixe have been identified and plasmid DNA has been purified from the corresponding bacterial colonies.

2.14 Plasmid DNA Mini- and Maxi-preparation

A single bacterial colony containing the plasmid DNA of interest was grown in a suitable volume of LB (4-5 ml for Mini-preparation, 200-400 ml for Maxi-preparation) in the presence of the appropriate antibiotic shaking at 37°C overnight. The Sigma-Aldrich Plasmid Purification kit, based on alkaline lyses method, was used to isolate the plasmid DNA from the cells according to the manufacture‘s instruction.

2.15 Sequencing

The DNA sequences have been obtained using the Automated Capillary Electrophoresis Sequencer 3730 DNA Analyzer (Applied Biosystems, Foster City, CA) by the Molecular Biology Service of the Stazione Zoologica A. Dohrn in Naples.

2.16 Oligonucleotides synthesis

All used synthetic oligonucleotides were prepared with a Beckman SM-DNA Synthesizer at the Molecular Biology Service of the Stazione Zoologica A. Dohrn in Naples.

2.17 Digested plasmids purification

To eliminate protein contaminations, the plasmid DNA linearized in order to obtain the template for riboprobes synthesis has been purified with 1 volume of phenol:chloroform:isoamylic alcohol (25:24:1), vortexed vigorously and centrifuged at 13000 rpm for 5' at 4°C. The soluble phase has been recovered and 1 volume of chloroform : isoamylic alcohol (24:1) has been added; the sample has been vortexed vigorously and centrifuged at 13000 rpm for 5', at 4°C. The aqueous phase has been recovered and the DNA has been precipitated adding 3 volumes of ethanol 100% and 1/10 volumes of Sodium acetate 3M pH 5.2. The sample has been mixed and stored over night at -20°C or 1 hour at -80°C. Then, it has been centrifuged at 13000 rpm for 15', at 4°C. The precipitated DNA has been washed with ethanol 70% (sterile or DEPC-treated), centrifuging at 13000 rpm for 15' at 4°C. The ethanol has been removed and the sample has been air-dried at R.T. At the end, the DNA has been diluted in a suitable volume of H2O (sterile or DEPC-treated), and its concentration has been evaluated by gel electrophoresis, using 1X Lambda DNA/Hind III Marker 2 (Fermentas), and using a spectrophotometer (Nanodrop 1000, Thermo SCIENTIFIC), reading the values at the wavelengths of 230, 260 and 280 nm and calculating the ratio between 260/230 nm and 260/280 nm to ascertain respectively the absence of chemical (phenol, ethanol) and protein contamination.

2.18 Ribonucleic probes preparation

2.18.1 RNA labelling

The plasmid, containing the template to be transcribed, has been conveniently digested and purified, as described above. 1 µg of purified, linearized DNA has been used as template for the ribonucleic probe synthesis. This template has been added to the following reaction mix: transcription buffer (1/10; Roche); Digoxigenin or Fluorescein labeling mix, containing 1 mM of ATP, CTP and GTP, 0.65 mM UTP and 0.35 mM DIG-11-UTP or 0.35 mM fluorescein-12-UTP (Roche); Sp6 or T7 RNA polymerase (2U/µl; Roche); Protector RNase inhibitor (1U/ µl).

The reaction has been performed in a total volume of 20 µl (in H_2O DEPC-treated). The mix has been briefly centrifuged and incubated for 2 hours at 37°C. Then, DNaseI RNase free (0.9U/µl) has been added in order to remove the DNA template. The sample has been incubated for 20' at 37°C. Finally, the reaction has been stopped adding EDTA pH 8.0 (16 mM). The synthesized ribonucleic probes have been purified using the mini RNeasy mini kit (QIAGEN), following manufacturer instructions. The ribonucleic probe quality has been checked by gel electrophoresis and the concentration quantification has been evaluated by Dot Blot analysis (see the next paragraph). One volume of deionized formamide has been added to the recovered samples, immediately stored at -80°C till the use.

The ribonucleic probes listed (**Table 2.1**) have been synthesized starting from cDNA clones present in N. Satoh *C. intestinalis* gene collection 1, available in the laboratory.

Table2.1 Genes of which ribonucleic probes have been synthesized

Gene name	Corresponding clone in N. Satoh gene collection 1	Probe lenght
Ci-gsx	citb029c24 (plate: R1CiGC31m18)	1250 bp
Ci-Meis	citb035l22 (plate: R1CiGC32a16)	1995 bp
Ci-Foxb	cilv039e20(plate: R1CiGC28o19)	1509bp

2.18.2 Ribonucleic probes quantification by Dot Blot analysis

The concentration evaluation of the DIG-11-UTP or fluorescein-12-UTP incorporated in the ribonucleic probes has been estimated making serial dilutions of the sample ribonucleic probes and of a Control RNA of reference (Roche), in a buffer containing DEPC-treated H_2O, 20x SSC, formaldehyde (5:3:2). 1 µl of each dilution has been blotted on a membrane Hybond-N (Amersham) and air-dried at R.T. The RNA has been UV-crosslinked on the membrane with a Stratalinker for 30". The membrane, with the UV-cross-linked RNA on it, has been washed in blocking solution (5% BSA

in 0.1 M maleic acid pH 7.5), for 30', shaking at R.T. Subsequently, the membrane has been incubated with anti-DIG or anti-Fluo phosphate alkaline antibody (0.15 U/ml; Roche) in blocking solution for 1 hour, shaking at R.T. To remove unbound antibodies, the membrane has been washed twice in a solution containing 0.1 M maleic acid pH 7.5 and 0.15 M NaCl for 15', at R.T. The membrane has been equilibrated in the detection solution (100 mM NaCl; 100 mM Tris pH 9.5; 50 mM MgCl2, in H2O) for 5', at R.T., and then incubated in the dark in the same solution in which Nitro-Blue Tetrazolium Chloride (NBT; 35 µg/ml) and 5-Bromo-4-Chloro-3'-Indolylphosphate p-Toluidine (BCIP; 175 µg/ml) have been added. The reaction has been monitored every 4-5' and blocked at the suitable moment, putting the membrane under running water. The membrane has been dried on 3MM paper and the concentration of the DIG-11-UTP or fluorescein-12-UTP incorporated in the ribonucleic probes has been calculated from the comparison with the control RNA spots.

2.19 Fluorescent report assays

Transgenic embryos, electroporated with constructs containing fluorescent reporters downstream of specific lineage promoters, were fixed at the desired developmental stage. Embryos were collected in 1,5 ml eppendorf tube pretreated with 2%BSA in MFSW and then washed to prevent them to stick to the walls. Embryos were prefixed in a solution containing in a 1:1 ratio of 4% paraformaldehyde, 0.1 M MOPS pH7.5, 0.5 NaCl and MFSW. Once the embryos settled completely the superrnatant was removed and replaced with a mixture containing 4% paraformaldehyde, 0.1 M MOPS pH7.5, 0.5 NaCl. Embryos were fixed for 30’ at R.T., then washed 3/5 times with PBS and stored at 4°C until confocal observations.

2.20 Whole Mount In situ Hybridization (WMISH) assays

2.20.1 Embryos preparation

Wild type or transgenic embryos at suitable embryonic stages have been fixed at R.T. for 90' or at 4°C over night, in a mixture containing 4% paraformaldehyde, 0.1 M MOPS pH7.5, 0.5 NaCl. Subsequently they have been washed three times in PBS 1x and dehydrated in graduated scale of ethanol (30% - 50% - 70% ethanol in distilled water DEPC-treated). They have been stored at -20°C until used.

2.20.2 WMISH protocol for single and double in situ

Day 1. The dehydrated stored embryos have been firstly re-hydrated in a graduate scale of 100% - 70% - 50% - 30% methanol in PBT (that is PBS + 0.1% tween 20), one wash of 20' for each methanol solution.

After that, the samples have been washed 3x15' in 1 ml PBT at R.T. and incubated 30' at 37°C in 1 ml PBT containing 2 µg/ml protease K for dechorionated embryos or 4 µg/ml for non dechorionated embryos, to increase the permeability to the cells and accessibility to mRNA target. The reaction has been stopped by a wash in 2mg/ml glycine in PBT. After digestion, samples have been post-fixed 1 hour at R.T. in 4% PFA+0.05% tween-20 in PBS 1x and then washed 3x15' in PBT. Embryos have been placed 10' in the pre-hybridization solution (50% formamide, 6x SSC, 0.05% tween 20) and finally 2 hour at 55°C in hybridization solution (50% formamide, 1x Denhardt‘s solution, 6xSSC, 0.05% tween 20, 100 µg/ml Yeast tRNA, 0,005% Heparine). Riboprobe (or Riboprobes for the double *in situ* hybridization) has been added up to a final concentration of 0.5 ng/µl and the hybridization occurred over night at the same temperature.

Day 2. A series of washes have been carried out by varying the temperature and salinity conditions; embryos have been, in fact, washed at 55°C in the following solutions: two times for 20' in Washing

Buffer 1 (WB1: 50% formamide, 5x SSC, 0,1% SDS), two times for 20' in WB1:WB2 and two times for 20' in WB2 (50% formamide, 2x SSC, 0,1% Tween 20). Subsequently they have been treated with a 1 ml Solution A (10mM Tris-Cl, pH8.0, 0.5M NaCl, 5mM EDTA, 0.1% tween), two times for 5' at R.T. To remove aspecific RNA, not bound to the corresponding endogenous mRNA, the embryos have been treated with RNase A (20 µg/ml) for 20' at 37 °C in solution A, then washed one time in WB3 (2x SSC, 0.1% Tween20) for 5' at R.T. and 2 times in WB3 at a temperature of 55°C. Following they have been incubated three times for 5' in TNT (0.1M Tris, pH 7.5, 150mM NaCl, 0.1% tween) at R.T.

At this point a slight difference in protocol for single or double *in situ* occurs.

For single *in situ* hybridizations, embryos have been incubated in Blocking TNB buffer (100mM Tris pH7, 150mM NaCl, 1% Blocking Reagent, 0.2% Triton-100x) for 2 hours at R.T. At this point embryos have been incubated, all night at 4°C, with the antibody anti-DIG in the ratio 1:2000 in Blocking TNB Buffer.

For double *in situ* hybridizations, embryos have been first incubated in TNB blocking buffer for 2 hours at R.T. too. At this point samples have been incubated over night at 4°C, with anti-DIG Fab Fragments POD HRP diluted 1:400 in Blocking Buffer TNB.

Day 3. For single *in situ* hybridizations, the samples have been washed at R.T. in TNT with the following modalities: one time for 5', four times for 20', one time for 40' and three times for 10' in TMN (100mM NaCl, 50mM MgCl2, 100mM Tris-Cl, pH9.5, 0.1% Tween20). To identify the localization of the RNA of interest, labeled with DIG and recognized by anti-DIG alkaline phosphatase conjugated, are provided the appropriate substrates that will be converted by the phosphatase in a precipitate of blue.

The embryos are incubated, therefore, in 1 ml of TMN containing 4.5 µl of nitroblue tetrazolium (NBT) and 3.5 µl of 5-bromo-4-chloro-3-indolyl-phosphate (BCIP). The time of formation of the precipitate are conditioned by the amount of antibody bound and, therefore, indirectly on the type of

probe used. For this reason, at intervals of 30' a few embryos are taken and observed, after being placed on a microscope slide, with a phase contrast microscope. When some signal was shown, the color reaction is stopped using 1x PBT.

Also for double *in situ* hybridizations series of washes were carried out: four times for 15' and two times for 5' in TNT at R.T. To identify the localization of the RNA of interest marked with Digoxigenin and recognized by anti-DIG conjugated to alkaline peroxidase (HRP) a substrate is converted by HRP in fluorescent product. The embryos have been incubated, therefore, in the 1x Plus Amplification Diluent (Perkin-Elmer) for 1' at R.T. and subsequently 1:400 Cy3 diluted in the same solution for 1.5 hours at R.T.

After the reaction, embryos were washed nine times for 5' in TNT at R.T. In order to stop the first antibody reaction an incubation in 50% formammide, 2x SSC, 0,1% tween-20 for 10' at 55°C has been performed. The next step consisted in a series of three washes of 10' in TNT and incubates, overnight at 4°C, with anti-Fluorescein HRP diluted 1:400 in Blocking Buffer TNB.

Day 4. (only for double *in situ*). The embryos have been washed two times for 5' in TNT at R.T., incubated in the 1x Plus Amplification Diluent (Perkin-Elmer) for 15' and subsequently treated with 1:400 Cy5 diluted in the same solution for 1.5 hours. Then the reaction has been blocked by carrying out the following washings: 1 time for 5' and 7 times for 10' in TNT at R.T.

Embryos were treated three times for 5 minutes and then over night with 1:10000 DAPI in TNT, in order to highlight the nuclei of the cells.

Single or double *in situ* hybridization experiments have been conducted at least three times independently, using a minimum of 25 embryos in each case. WMISH conducted on electroporated embryos were considered reliable when consistent in at least 60% of the analyzed embryos.

2.21 Preparation of constructs

Different constructs were already available in the Laboratory or prepared during this study, by cloning strategies illustrated below.

- *pGsx>GFP* (Fig. 2.1) was already available in Laboratory and it contains a Gsx cis-regulatory region (*pGsx>GFP*) of about 2.8 Kb cloned upstream from GFP. To prepare this construct *Ci-gsx* regulatory region, *pGsx*, was previously obtained by PCR amplification on genomic DNA and the amplified product, digested with HindIII/NotI, was inserted upstream of GFP in the pTyrp1/2a>GFP vector, available in laboratory, previously digested with HindIII/NotI to eliminate pTyrp1/2a.

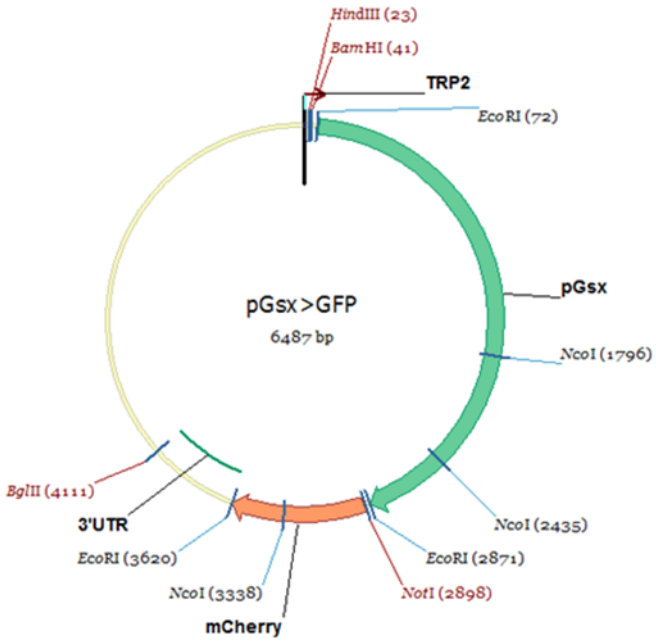

Fig. 2.1 Map of pGsx>>GFP vector

- pGsx-0,39>LacZ was available in the laboratory and it contains a minimal regulatory element of Gsx (pGsx-0,39) responsible for its expression since the neural plate stage cloned upstream of Nuclear Localization Signal (NLS)/LacZ.

For photoreceptor analyses we exploited or modified a number of constructs, pZicL/H2B/mCherry, pDMRT/H2B/YFP, pFoxB/UNC76/GFP (Fig. 2.2) kindly provided by Albero Stolfi, a postdoctoral researcher in the laboratory of Dr. Lionel Christiaen at New York University.

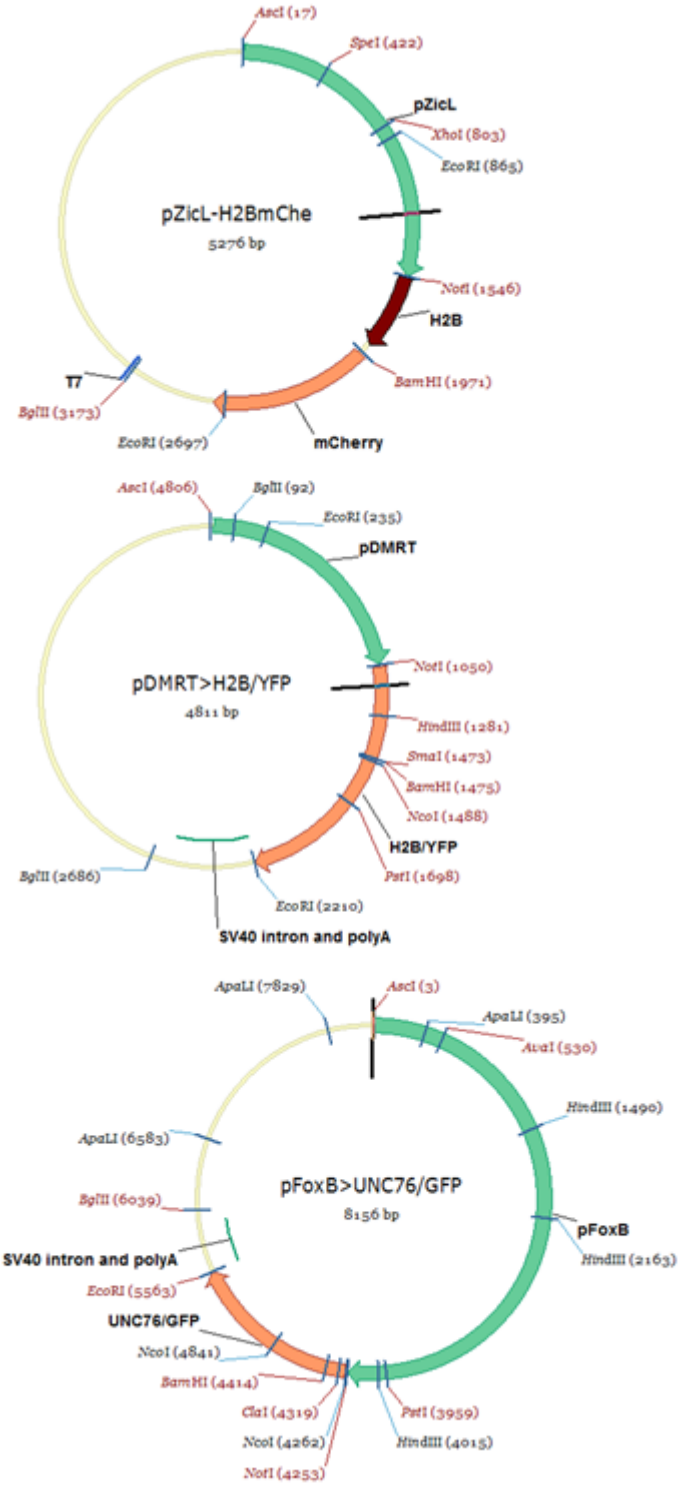

Fig. 2.2 Map of pZicL/H2B/mCherry, pDMRT/H2B/YFP, pFoxB/UNC76/GFP

- *pDMRT>H2B>mCherry* and *pFoxb>H2B>mCherry*. To prepare these constructs, we excised the DMRT and FoxB promoters, by AscI/NotI digestion, respectively from pDMRT/H2B/YFP and pFoxB/UNC76/GFP constructs, and inserted pDMRT and pFoxB upstream of H2B>mCherry in the pZicL/H2B/mCherry vector, previously digested with AscI/NotI to eliminate ZicL.
- *pFoxb>H2B>YFP.* To prepare this construct, we removed pFoxB promoter, by AscI/NotI digestion, from pFoxB/UNC76/GFP and inserted pFoxb upstream of H2B>YFP in the pDMRT/H2B/YFP vector, previously digested with AscI/NotI to eliminate pDMRT.
- *pGsx>H2B>mCherry*. To prepare this construct, we removed GFP from pGsx>GFP construct, by NotI/BglII digestion, and replaced it with H2B/MCherry removed from pZicl>H2B>mCherry by NotI/BglII digestion.
- *pTH>GCaMP*. pGP-CMV-GCaMP6s (ID 40753) plasmid was purchased from Addgene (www.addgene.org) and the region containing GCaMP was amplified by PCR using primers AMP6- AMPR (see **Table 2.4**) bringing restriction sites for SpeI (actagt) and EcoRI (gaatcc), respectively at the 5' and 3' ends. 5 µl of PCR product were run on a agarose 1% gel to test amplification efficiency and then the resultant 45 µl were purified using The QIAquick PCR Purification Kit (Quiagen). The purified PCR product was double digested with SpeI/EcoRI and then extracted from 1% agarose gel. In parallel the pTH promoter was amplified by PCR, from the contruct pTH>Kaede (kindly provided by Florian Razy-Krajka), using primers that include the restriction sites for AscI (pTHa) at the 5' end and SpeI (pTHs) at the 3' end (see **Table 2.4**). The backbone for the final construct was provided by pZicl>H2B>mCherry which was digested AscI/EcoRI to remove pZicl>H2B>mCherry and to insert pTH (AscI/SpeI) and GCaMP (SpeI/EcoRI) in a triple ligation reaction. The resultant colonies were screened by PCR using internal oligos (AmpRC-pTHfc, see **Table 2.4**). Miniprep of positive clones were

prepared and sequenced with the same oligos used for the PCR screening. Clones were selected from the positive sequences to produce maxiprep.

Table 2.2: list of oligonucleotides used for pTH>GCaMP cloning

Amp6	**5'-GCCATGACTAGTCGCCACCATGGGTTCTCA-3'**
Ampr	**5'-CTGAATTCTCACTTCGCTGTCATCATT-3'**
pTHa	**5'-CTTGGCGCGCCTTTGTTGCAGAGCAGCTCATGAT-3'**
pTHs	**5'-TGACTAGTTCAGTGCTTAGACTTAGCTGG-3'**
AmpRC	**5'-GTCGGCCTTGATATAGACG-3'**
pTHfc	**5'-ACGATGTTGTAAGAATTTGCGA-3'**

- *pTh>H2B>mCherry*. TH promoter was amplified from pTH-Kaede with primers designed to add restriction sites for AscI (pTHa) and NotI (pTHNR) at the 5' and 3' ends respectively (see **Table 2.5**). The pPCR purified product, after being checked on 1% agarose gel, was double digested AscI/NotI and inserted in the pZicl>H2B>mCherry construct, previously digested with AscI/NotI to remove the Zicl promoter.

Table 2.3: oligonucleotides used for pTH>H2B>mCherry cloning

pTHa	5'-CTTGGCGCGCCTTTGTTGCAGAGCAGCTCATGAT-3'
pTHNR	**5'-CTTGCGGCCGCTTCAGTGCTTAGACTTAGC-3'**

- Other constructs (pZicl>Ets>WRPW, pZicl>Ets>VP64 pZicl>Elk>WRPW, pZicl>Ets>VP64, pFog>Nodal, pFog>Delta-like), used in this study, were kindly provided by Drs. Clare Hudson and Hitoyoshy Yasuo. pARR-eGFP was kindly provided by Dr. Kusakabe (Department of Life Science, Graduate School of Science, Himeji Institute of Technology).

2.22 *In silico* analysis of putative *trans*-acting factors

The pGsx-0.39 sequence was submitted to JASPAR database (http://jaspar.genereg.net/) and the Genomatix Database (http://www.genomatix.de/cgi-bin/eldorado.main.pl), using in both cases the default parameters. These are databases of transcription factor from many organisms, their genomic binding sites and DNA-binding profiles. The analysis revealed the the presence of several potential binding sites for Ets TFs family, scattered along the pgsx-0.39 sequence (Fig. 3.7). Three of them were classified as Elk1/3/4 binding sites (El1,El2,El3 in yellow) and the other three were classified as general Ets binding sites (E1,E2,E3 in pink). The exhaustive analysis permitted to identify two fundamental sites for the activation of pGsx-039 promoter, namely El2 and E2. Constructs in which each Ets/Elk binding sites were mutated have been prepared using the QuikChange® Site-Directed Mutagenesis Kit "Stratagene" from *pGsx-0.39>LacZ* construct. The oligo used for the mutation of the putative Elk (El2) and Ets (E2) binding site involved in Gsx activation have been replaced by a sequence that reduced the binding affinity, by using mutagenic oligonucleotides of about 50 bp, listed in ***Table 2.6***. According to the manufacturer's instruction, these mutated oligonucleotides have been used for a PCR reaction using as template *pGsx-0.39>LacZ*.

The PCR reaction has been carried out using PFU DNA polymerase, and these cycling parameters:

- First step (1 cycle). DNA denaturation: 30" at 95°C.
- Second step (repeated for 18 cycles).

  DNA denaturation: 30" at 94°C.

  Oligonucleotides annealing: 1' at 55°C

  Polymerization: 68°C for 7'.

The presence of amplified product has been checked on 1% agarose gel. At this point, to eliminate the wild type plasmid, used as template, the mixture has been digested at 37°C for 1.5 hour, with 1 µl of the *Dpn*I restriction enzyme (10 U/µl). This enzyme digests only the methylated supercoiled

dsDNA used as template, but not the newly synthesized mutated and unmethylated DNA. After the digestion, an aliquot of the reaction has been transformed and grown as previously described. Ten clones have been selected after growth; the isolated plasmids have been sequenced to check the presence of mutations.

In ***Table (2.6)*** the mutagenic oligonucleotide sequences are reported. The wild type sequence for each putative binding site is indicated as wt (wild type); putative Ets/Elk binding sites are highlighted in green and and the corresponding mutated sequences are indicated in red.

The double mutant for El1/E2 binding sites, was obtained by mutating E2 on the single mutant Mut/E11>LacZ.

Table 2.4: Mutagenic oligonucleotides

Wt El2	5'-CAAGTGGAACGCGCTGCTGATTTCACTTCCCTGGTCTCCAACTG-3'
MutEl2F	**5'-CAAGTGGAACGCGCTGCCCAGGGCACTTCCCTGGTCTCCAACTG-3'**
MutEl2R	5'-CAGTTGGAGACCAGGGAAGTCCCTGGGCAGCGCGTTCCACTTG-3'
Wt E2	**5'-GGCGATCCGGGGTTCGATATTTCCCATGGTCGGCGCTGCTAGATCGCGA-3'**
MutE2F	5'-GGCGATCCGGGGTTCGATATAGCGCGACCCCGGCGCTGCTAGATCGCGA-3'
MutE2R	**5'-TCGCGATCTAGCAGCGCCGGGGTCGCGCTATATCGAACCCCGGATCGCC-3'**

2.23 Chemical inhibition

The strategies adopted to interfere with the signaling patwhays active on neural plate included also the chemical inhibition. Embryos at different developmental stage were treated with specific drugs able to inhibit each considered pathway.

In particular for Nodal, the embryos were treated with SB431542 (Tocris), a pharmacological inhibitor of the TGFβ type I receptors ALK4/5/7 (Inman et al., 2002). This inhibitor blocks the receptors, for Activin and Nodal ligands, without inhibiting other ALK family members binding other ligands (Inman et al., 2002). SB431542 was added to dechorionated embryos at the developmental stage of 16-cells, in a final concentration of 5 μM starting from a stock solution of 25 mM.

To interfere with delta/notch signaling the embryos were treated with DAPT (Calbiochem), inhibitor of gamma-secretase, an enzime necessary for the Notch receptor processing. DAPT was dispensed to dechorionated embryos at the 110 cells stage. The working solution was 100 μM starting from a stock solution of 100 mM.

The chemical inhibition of FGF was performed using the molecule U0126 that specifically blocks MEK/ERK (Duncia et al., 1998). U0126 was added to dechorionated embryos at the 110 cells stage. The stock solution was 100mM while the working concentration was 4 μM.

The embryos treated were washed in MFSW several times at gastrula stage then were fixed for WMISH at late gastrula and neurula stages.

2.24 Pressure test

To characterize animal behaviour, wild type animals were put in a recording chamber designed by Dr Bezares-Calderón LA. The chamber consists of a box of the following dimensions (width×depth×length=25·mm×100·mm×70·mm). The main frame is made of steel. On front and lateral sides there are glass screen, while the other sides are made of dark plastic material. To increase pressure air was directly inflated into the chamber by a sealed hole on the lid. The lid was placed on the rest of the chamber and tightly screwed to prevent air dispersal. The air was provided by a pressurized air system directly connected to two valves (an increase valve to pressurize the chamber and a release valve to restore normal pressure levels) and a manometer to measure exactly the added pressure. The chamber is filled until 80% of the volume with MFSW containing larvae and the remainig with air. The illumination was provided by both lateral sides by nonactinic far-red photodiodes (wavelength 640 nm).

2.24.1 Hydrostatic pressure changes

The Hydrostatic pressure inside the chamber was increased providing pressurized air. The pressure changes were finely controlled by the manometer outside the chamber. The experimental conditions

were: 30seconds before stimulation, 90 seconds of pressure increase of 1bar and 30 seconds of pressure release. The normal pressure level was rapidly reached simply opening the restore valve.

2.24.2 Define Interval of response

The first step of this analysis was to define the developmental window in which the hydrostatic pressure response is considerable. Then three different wild type batches were analyzed indipendently in the pressure chamber designed by Dr. Bezares. Starting from 30' after hatching animals were placed at 1h interval in the chamber, their swimming behavior was recorded and then placed back in a glass beaker at 18°C.

2.24.3 Characterize the pressure behaviour

Six indipendent experiments were conducted to define the hydrostatic pressure response. The behavior of wild type larve was recorded at 1,5h post-hatching. The recording schedule is divided in 30s no pressure, 90 seconds pressure increase of 1 bar and then 30 seconds pressure release.

2.24.4 Recording

The animal movements were recorded, for the above mentioned time interval, in the chamber by a camera from Imagin Source (DMK 42BUC03) recording in 8 bit at a resolution of 1280x 960 pixel (1.2MP) up to 25fps and sensible to IR illumination. To the camera is attached a 1/3" lens from Computar (HG1214FCS-L) the focal lenght is 4mm and the aperture is f1,2. Thanks to the nonactinic far-red illumination from both sides animals appear as white spots on the dark background. The focus was tuned each time manually, while the exposure and the gain was determined before recordings and fixed as default to reduce video variability. All the recording were performed in a dark room at 18 °C. The recording software is IC Capture from imaging source.

2.24.5 Tracking

The resultant movie from each recording was analysed by image j to track the animal movements and extrapolate spatial parameters. The raw videos were analyzed according to the script develped by Dr. Martin Gühmann. The raw video is splitted in smaller fragments of 30 frames (2 seconds) to facilitate the analysis. Then the background is calculated and subtracted to each frame. The video is than inverted so the animals now appear as black dots in a white background, this is useful to speed up the tracking because the software has to consider less moving objects. The resultant video is then tresholded. The last step is to subject the videos to the mTrack2 plugin. The plugin analyze the videos and gives back a list of spatial parameters from wich the larvae movements were extrapolated and plotted.

2.24.6 In vivo imaging

To test in vivo calcium imaging animals were put in another device developed by Dr Bezares-Calderón LA. It consisted in a chamber that fits into the holding tray of the confocal microscope. That device has a cavity in the middle connected by two openings through wich is possible to increase pressure inflating pressurized air. The animals are attached on a round cover slip by gluing their tail in a drop of glue dispersed in a small volume of MFSW. The cover slip is then reversed to the chamber enabling the glued animal to face the cavity and tightly screwed. The animals undergo confocal microscopy analysis. The GCaMPs consist of a circularly permuted enhanced green fluorescent protein (EGFP), which is flanked on one side by the calcium binding protein calmodulin and on the other side by the calmodulin binding peptide M13 (Nakai et al., 2001). In the presence of calcium, calmodulin-M13 interactions elicit conformational changes in the fluorophore environment that lead to an increase in the emitted fluorescence (Nakai et al., 2001; Tian et al., 2009). To detect the fluoresce increase the animals were subjected to a z-scan analysis in three conditions: prior to pressure stimulation, 1bar pressure increase and pressure release.Since the signal coming from GCaMP fusion protein was not always detectable to focus on coronet cells the animals were

coelectroporated also with pTH>H2B>mCherry. The resultant images were processed by image j to generate a z-projection with maximum intensity. The imagese were presented as 16 colors heatmap that reflected the fluorescence intensity. The resulting intensities of each condition were then compared to test whether there is an appreciable change in GFP signal among them subsequently to a calcium increase reflecting neuronal activity.

Bibliography

Duncia, J.V., Santella, J.B., 3rd, Higley, C.A., Pitts, W.J., Wityak, J., Frietze, W.E., Rankin, F.W., Sun, J.H., Earl, R.A., Tabaka, A.C., Teleha, C.A., Blom, K.F., Favata, M.F., Manos, E.J., Daulerio, A.J., Stradley, D.A., Horiuchi, K., Copeland, R.A., Scherle, P.A., Trzaskos, J.M., Magolda, R.L., Trainor, G.L., Wexler, R.R., Hobbs, F.W., Olson, R.E., 1998. MEK inhibitors: the chemistry and biological activity of U0126, its analogs, and cyclization products. Bioorg Med Chem Lett 8, 2839-2844.

Inman, G.J., Nicolas, F.J., Callahan, J.F., Harling, J.D., Gaster, L.M., Reith, A.D., Laping, N.J., Hill, C.S., 2002. SB-431542 is a potent and specific inhibitor of transforming growth factor-beta superfamily type I activin receptor-like kinase (ALK) receptors ALK4, ALK5, and ALK7. Mol Pharmacol 62, 65-74.

Nakai, J., Ohkura, M., Imoto, K., 2001. A high signal-to-noise Ca(2+) probe composed of a single green fluorescent protein. Nat Biotechnol 19, 137-141.

Tian, L., Hires, S.A., Mao, T., Huber, D., Chiappe, M.E., Chalasani, S.H., Petreanu, L., Akerboom, J., McKinney, S.A., Schreiter, E.R., Bargmann, C.I., Jayaraman, V., Svoboda, K., Looger, L.L., 2009. Imaging neural activity in worms, flies and mice with improved GCaMP calcium indicators. Nat Methods 6, 875-881.

Chapter 3

Results and Discussion

3.1 Generation of cell diversity in *Ciona* CNS: Neural Plate a-Lineage Row III Patterning

To study the molecular mechanisms involved in the patterning of a-lineage row III blastomeres, we interfered with the Nodal and Delta/Notch signaling pathways in different ways, as chemical inhibition, injection of anti-sense morpholino oligonucletides (MO) and transgene overexpression. To follow the patterning of each blastomere, I carried out in situ hybridization experiments by using a set of three genes, *Trp*, *Gsx* and *Meis*, which label row III cells in columns 3 (lateral), 2 (intermediate), and 1 (medial), respectively, at neurula stages. The expression of *Trp* and *Meis* was checked at neurula stage (8h of development at 18°C) when neural plate blastomeres have divided along A-P axis. *Gsx* expression was analyzed in embryos at slightly earlier neurula stage (7,5h of development at18°C) because later *Gsx* starts to be expressed also in column 1. The MO injection experiments were carried out by Yasuo group in Villefrance, whereas chemical inhibition, transgene overexpression and in situ hybridization experiments were shared between Yasuo and our laboratory. This part of my thesis work has been recently published (Esposito et al., 2017).

3.1.1 Nodal signalling and lateral patterning

Nodal is expressed in the b-lineage cells adjacent to the most lateral a-lineage precursors since 32-cell stage (Fig. 3.1).

To inhibit Nodal activity, embryos were treated with the pharmacological inhibitor SB431542 (inhibitor of TGFβ type I receptors ALK4,5,6) or injected with Nodal antisense morpholino oligonucleotide (Nodal-MO). Both treatments resulted in loss of Trp expression from column 3. *Gsx* expression in column 2 was also strongly reduced following Nodal signal inhibition.

Fig. 3.1. Expression patterns of Nodal. *Schematic drawings showing sequential activation of Nodal during the 32-cell stage to 6-row neural plate stage. Gene expression is indicated by black dots, with weaker expression represented by grey dots. The a-lineage neural plate cells that generate the CNS are colored in red.*

However, in many embryos endogenous *Gsx* expression was lost from column 2 and was ectopically present in column 3. This data indicate that Nodal is involved in activation of *Gsx* in column 2 and, at the same time, in *Gsx* inhibition in column 3. *Meis* was ectopically expanded in column 2 (88% of nodal MO; 96 % of SB treated embryos) and in column 3 (18% of nodal MO; 27 % of SB treated embryos) (Fig. 3.2). Hence, the data indicates that *Nodal* is required for the correct specification of row III since it promotes column 3 identity (by activating *Trp* and repressing *Gsx*), column 2 identity (by activating *Gsx*) and represses medial column gene expression (by repressing *Meis*) in lateral cells.

On the other hand, overexpression of *Nodal*, using the upstream regulatory sequences of *FOG* (*pFOG>Nodal*) to drive its expression throughout the animal hemisphere from the 16-cell stage of development (Hudson et al., 2015; Pasini et al., 2006; Rothbacher et al., 2007) resulted in opposite effects. Indeed, an ectopic expression of *Trp* and a loss of both *Gsx* and *Meis* expression was detected throughout the row III daughters (Fig. 3.2). This data indicate that *Nodal* is able to induce column 3 identity and repress column 1 and 2 identity.

Collectively, these experiments point to an important role played by *Nodal* in specifying columns 2 and 3 and in repressing column 1 identity.

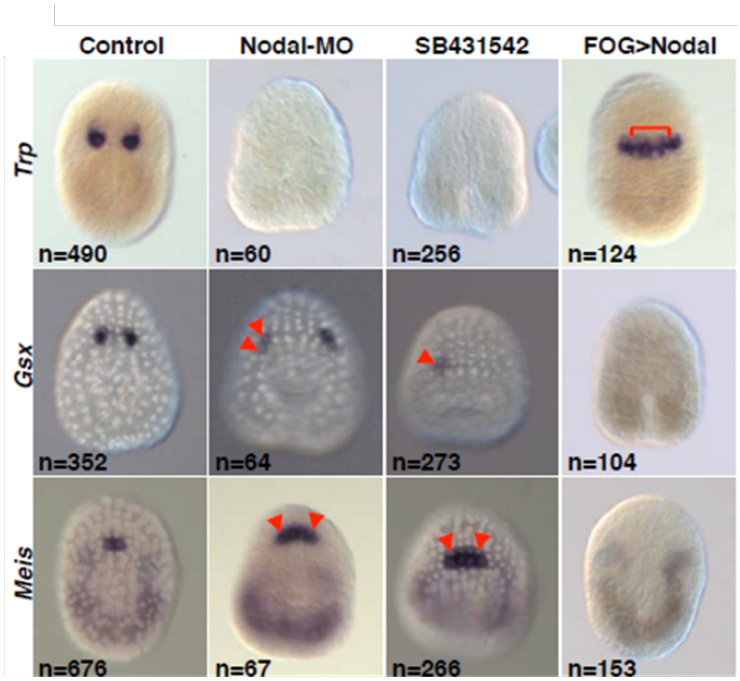

Fig. 3.2 Nodal pattern the a-lineage CNS precursors*. Markers analyzed are indicated to the left, embryo treatment indicated above the columns. All embryos are at neurula stage in dorsal view. Red arrowheads or brackets indicate ectopic expression. Some embryos are stained with DAPI to confirm cell identification. n= total number of embryos analyzed.*

3.1.2 Delta/Notch signaling in column 1 and 2 fates

Delta-like (previously *Delta2*) is one of the known target of Nodal signaling in *Ciona*. It is expressed in b-lineage neural precursors as well as in vegetal A-lineage cell at the 64-cell stage (Fig. 3.3) At the early gastrula stage, *Delta-like* is expressed in the lateral A-lineage neural precursors and b-line cells and later, at neural plate stage, it is expressed in the lateral borders of the neural plate (Fig. 3.3).

Fig. 3.3. Expression patterns of Delta-like. *Schematic drawings showing sequential activation of Delta-like during the 32-cell stage to 6-row neural plate stage. Gene expression is indicated by black dots, with weaker expression represented by grey dots. The a-lineage neural plate cells that generate the CNS are colored in red.*

Notch receptor transcripts are instead present ubiquitously during early cleavage stages with expression detected from the late gastrula stage in the developing nervous system (Imai et al., 2004). To inhibit Delta-like/Notch signaling, I treated the embryos from the 76-cell stage with DAPT, an inhibitor of gamma-secretase, an enzyme required for Notch receptor processing. A further way to interfere with the signaling involved the injection of mRNA coding for a dominant negative form of Suppressor of Hairless, a transcription factor known to mediate Notch signaling. In both cases, I observed a strong reduction in *Gsx* expression and concomitantly, an ectopic expression of *Meis* in column 2 (Fig. 3.4). On the other hand, overexpression of *Delta-like,* by electroporation of the construct *pFOG>Delta-like*, induced an opposite effect, means that the expression of *Meis* was completely lost and *Gsx* was ectopically expressed in column 1 (Fig. 3.4).

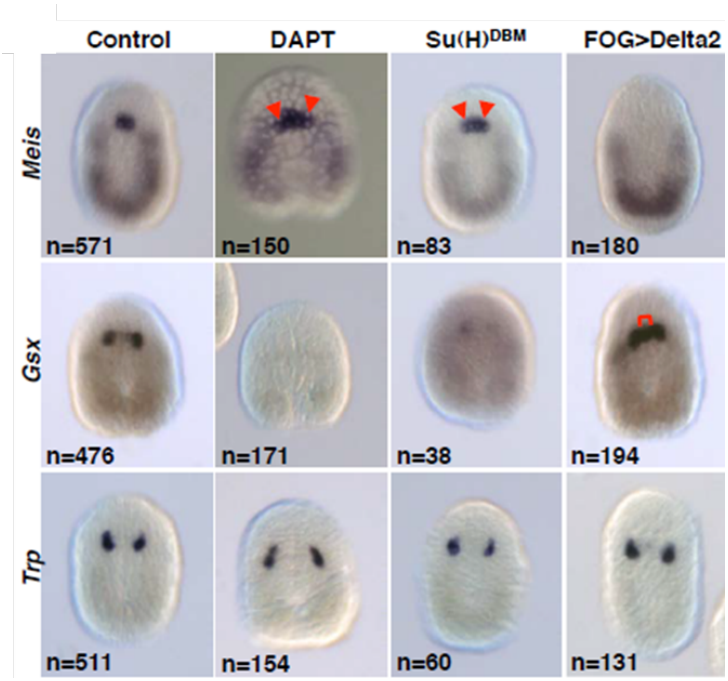

Fig. 3.4 Delta/Notch pattern the a-lineage CNS precursors. *The markers are indicated to the left, embryo treatments above the columns. All embryos are at neurula stage in dorsal view. Red arrowheads or brackets indicate ectopic expression. n= total number of embryos analysed.*

Thus, it appears that Delta-like/Notch signals promote column 2 fates at the expense of column 1 fates in the a-lineage neural plate.

3.1.3 FGF and anterior-posterior patterning of a-lineage row III

One of the signaling molecule playing a fundamental role in *Ciona* CNS development is the Fibroblast growth factor (FGF) signaling, which is responsible for early neural induction of a-line neural lineages since the 32-cell stage (Bertrand et al., 2003). The requirement for FGF signaling persists at the neural plate stage, when it acts to promote A-line row I fates and repress row II fates (Hudson et al., 2007), through a differential activation of Erk1/2 between row I (active) and row II (inactive). The same differential activation of Erk1/2 occurs also in a-line III/IV sister rows, where Erk1/2 is activated in row III and is inactive in row IV. Thanks to this mechanism, the most lateral a-cells row III, the a9.49 pairs (Fig. 1.8) are directed to the fate of otolith and ocellus pigmented cells, via the well known FGF downstream effector, Ets1/2 (Haupaix et al., 2014; Hudson et al., 2007; Racioppi et al., 2014; Squarzoni et al., 2011). Furthermore, more recently, it has been suggested that FGF signaling is involved also in specifying medial lineages of row III (a9.33 and a9.37), through two different Ets family transcription factors, Ets1/2 and Elk 1/3/4 (Gainous et al., 2015).

On these grounds, my next efforts were devoted to finding a direct relation between FGF and *Gsx*, the marker for the intermediate column of row III (a9.33 blastomere pair). As first approach, I used the pharmacological agent U0126, a known inhibitor of the MAP kinase kinase, MEK1/2. The results revealed that U0126 treatment almost completely abolishes *Gsx* expression in the neurulae (Fig. 3.5), compared to the controls. As already reported, previous studies in the Laboratory, done by the former PhD student Rosaria Esposito, permitted the identification of the minimal regulatory element of *Gsx* (*pGsx*-0,39) responsible for its expression since the neural plate stage. I thus treated with U0126 the transgenic *pGsx-0,39>LacZ Ciona* embryos, in order to analyse its effects on the regulation of *Gsx* expression. As for the endogenous *Gsx*, U0126 treatment resulted in block of LacZ expression *in pGsx-0,39>LacZ* transgenic embryos (Fig. 3.5), indicating FGF/MEK1/2 involvement in *Gsx* transcriptional regulation.

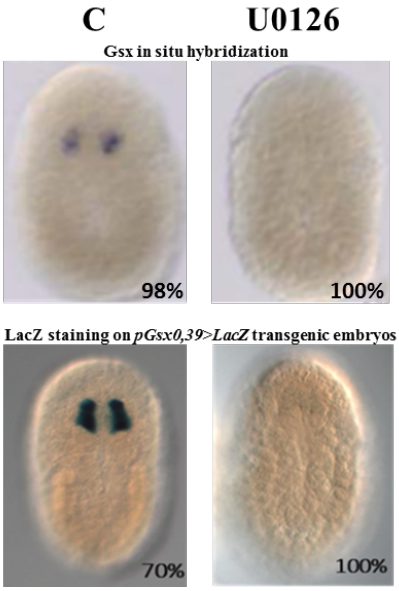

Fig. 3.5 Effects of U0126 on Gsx endogenous transcript and its regulatory region.

In the next step, I tried to address this question: which Ets family member, Ets1/2, Elk1/3/4 or both, translates FGF signalling and induces *Gsx* expression? To reach this goal, I exploited the constructs, available in the Laboratory, in which constitutively inactive and active forms of Ci-Ets1/2 (Ets:WRPW and Ets:VP64, respectively) or Elk1/3/4 (Elk:WRPW and Elk:VP64, respectively) transcripts are under the *ZicL* promoter (Shimai et al., 2010) (*pZicL/Ets:WRPW, pZicL/Ets:VP64, pZicL/Elk:WRPW, pZicL/Elk:VP64*). *ZicL* promoter is active in the neural lineage since the neural plate stage (Shimai et al., 2010).

The analysis showed that both constructs *pZicL/Ets:WRPW* and *pZicL/Elk:WRPW* behave almost similarly, in the sense that both led to a reduction of endogenous *Gsx* expression, while the use of *pZicL/Ets:VP64* and *pZicL/Elk:VP64* constructs did not result in any significant difference in the pattern of *Gsx* (Fig. 3.6).

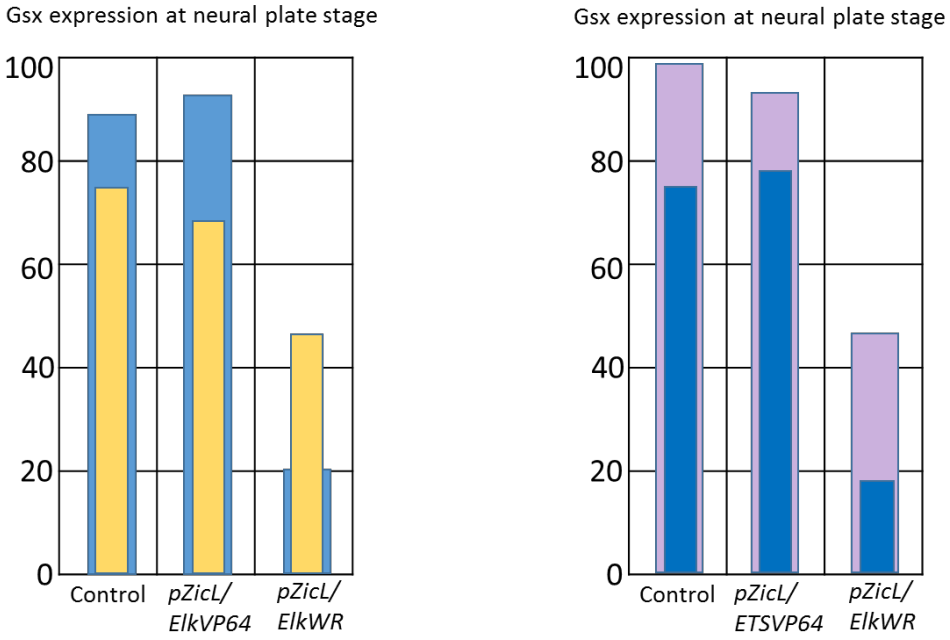

Fig. 3.6 Effects of interference with Ets/Elk factors on Gsx endogenous transcript. *The graphs indicate the percentage of embryos showing Gsx expression in each category. Two experiments (shown in two different colors) were done for each group (Ets and Elk) of transgenes.*

These results clearly show that both, Ets and Elk family members, are involved in the activation of *Gsx* in the neural plate.

The entire *pGsx*-0.39 region was thus subjected to bioinformatic analyses, in order to identify putative consensus binding sites for Ets family transcription factors. The bioinformatic analysis of *Gsx* promoter revealed the presence of several potential binding sites for Ets TFs family, scattered along the *pGsx-0.39* sequence (Fig. 3.7). Three of them were classified as Elk1/3/4 binding sites (El1,El2,El3 in yellow) and the other three were classified as general Ets binding sites (E1,E2,E3 in pink).

Fig. 3.7 Ets/Elk binding sites on pGsx-0.39 promoter fragment. *In yellow Elk and in pink Ets putative recognition sequences. The sites involved in Gsx activation are underlined.*

Taking into considerations the results obtained from different round of mutagenesis, in which I

mutated each binding site alone or in combination with others, this exhaustive analysis permitted to identify two fundamental sites for the activation of *pGsx*-039 promoter, namely El2 and E2 (Fig. 3.7, underlined). Indeed, as emerged from three experiments, in the double mutant El2+/E2 electroporated embryos only around 10% of them showed a conspicuous activation of the promoter, as revealed by LacZ staining, in the endogenous *Gsx* regions compared to around 70% of control embryos (+++ in Fig. 3.8A). Thus, it appears that Ets and Elk consensus binding sites are involved in the minimal promoter expression.

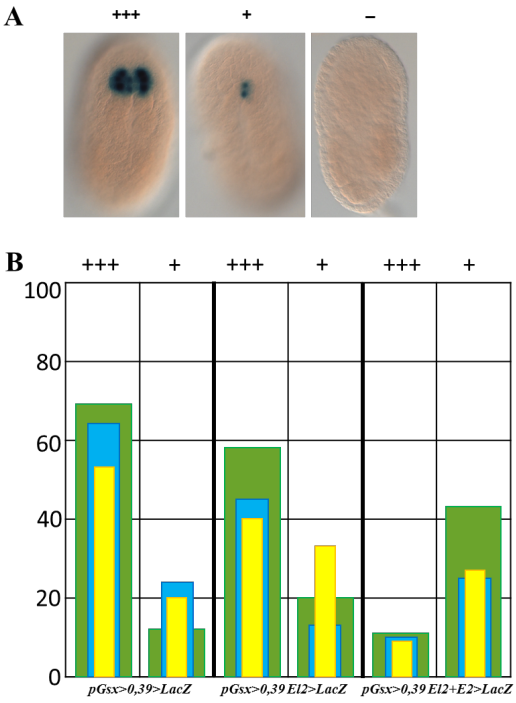

Fig. 3.8 Identification of Ets/Elk binding sites on Gsx promoter. *A) Representatives of Ciona neurula embryos showing strong (+++), low (+) and no (-) transgene expression after electroporation of the constructs of interest. B) Diagram illustrating the percentage of embryos, from three different experiments (color code), showing Gsx expression in each category*

3.1.4 Concluding Remarks

Collectively my data further confirm *Ciona* as a very useful model system to understand developmental strategies adopted in the lineage of chordates to shape the different body structures. In

particular, the neural plate shows a grid-like organization with only six rows and eight columns of aligned cells, in which each cell express specific markers at precise developmental times and can be easily identified, thus permitting to study cell fate diversification at the level of individual cells. This is a huge advantage, compared to the thousands of cells present in vertebrates, for studies aimed at investigating both the precise role played by each signalling pathway and transcription factor and, at the same time, their complex interplay in shaping the CNS.

My studies contributed to add a further stone to the neural plate mosaic, since Idemonstrated that, despite the distinct embryonic lineage origins within *Ciona* larval CNS, the mechanisms that pattern the posterior A-lineage and the anterior a-lineage neural precursor are remarkably similar. In this scenario, *Nodal* signalling is required for lateral neural plate fates and *Delta/Notch* refines the initial pattern established by *Nodal* and subdivide each of the lateral and medial domains to generate four columns. Superimposed on this mediolateral pattern is the FGF signaling, which induces differences in antero-posterior identities through the differential activation of Erk1/2 between rows I and II (A-lineage) and between rows III and IV (a-lineage). My data permitted also to collect further evidences on the mechanisms by which signalling pathways are integrated at the level of transcriptional control of cell-type-specific gene markers. Previous studies from my laboratory assigned a fundamental role to FGF signaling in pigment cell specification by directly activating Ci-TCF in the a9.49 cells (the most lateral a-lineage row III cells) through FGF downstream effector Ets1/2. In the course of my thesis work, by performing chemical and transgene-mediated inhibition, I collected evidences that FGF signaling pathway directly activates *Gsx* expression in the a9.33 cells (the intermediate a-lineage row III cells) through Ets1/2 and Elk1/3/4 factors. This is in line with recent data from Levine Lab (Gainous et al., 2015) which indicate that both Ets1/2 and Elk1/3/4 shows partially redundant activities in intermediate and medial lineages (a9.33 and a9.37) of row III.

Thus, FGF signaling is involved in *Gsx* activation. However, it is not hard to imagine that further mechanisms, besides FGF, are responsible for a so precise and definite expression, including

repressive mechanisms that block *Gsx* expansion in the lateral and anterior blastomeres. And indeed, data from Yasuo and my laboratory indicate that Snail and Msxb transcription factors are both required to repress *Gsx* expression in lateral column 3 (Esposito et al., 2017). Further studies are currently ongoing in the lab to reveal the molecule(s) responsible for blocking anterior expansion of *Gsx* and the related regulatory mechanisms.

3.2 Photoreceptor cells (PCRs) lineage

As previously mentioned, the developmental story of PRCs lineage is still debated. Initially it was suggested that PRCs originate from the right blastomeres a9.33 and a9.37 of the neural plate stage (Cole and Meinertzhagen, 2004). This was confirmed by later studies using Arrestin antibody (Horie et al., 2005). However, these data have been recently challenged, since it has been suggested that photoreceptor cells derive from more posterior regions of the neural plate, most likely medial regions of row II (Gainous et al., 2015). A further refinement of these studies indicated that the photoreceptor cells of the pigmented ocellus develop from the right A9.14 cell, while those of the non-pigmented ocellus develop from the right A9.16 cell (Oonuma et al., 2016).

As previously described, *Gsx* is firstly detected at the neural plate stage in the a9.33 blastomeres (Fig. 3.9 A,B yellow arrow) and, as development proceeds, a further signal appears more posteriorly ((Fig. 3.9 C,D green arrow) in a region that is likely to be part of A-lineage descendant.
To unveal if the *Gsx* later posterior emerging territories could mark the A-lineage progeny, double in situ hybridization experiments were carried out using *Gsx* in combination with *Ci-FoxB* probe at different developmental stages.

At neural plate stage *Gsx* expression is detectable in the a9.33 pair, while *FoxB* in the more posterior A-lineage row II, specifically in the A9.14 and A9.13 pairs (Fig. 3.10A). At the neurula stage, *Gsx* expands medially, in the a9-37 lineage, while *FoxB* elongates posteriorly (Fig. 3.10 B). As development proceeds a further *Gsx* signal appears more posteriorly in a region that is likely to be

part of A-lineage descendants and that overlaps with the anterior *FoxB* expression domains (turquoise arrow in Fig. 3.10 C, D, D', D''). Thus, it appears that *Gsx* in the early developmental stage is present in a-lineage territories and from late-neurula/early-tailbud stage it marks also the anterior A-lineage blastomeres, coinciding with anterior *FoxB* expression in the nervous tissues. This indicates that *Gsx* could represent a good marker for the "old" but also for the "revised" lineage of photoreceptor cells.

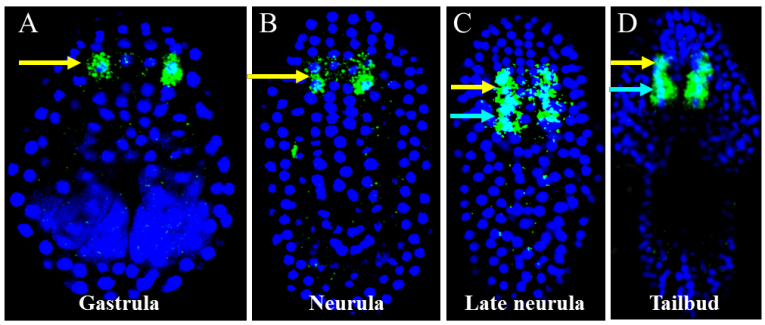

Fig. 3.9 Gsx in situ analysys. *Merged images, all in dorsal view, of Gsx WMISH, plus DAPI nuclear staining (in blue), at different embryonic stages, reported on the bottom of each picture row. Yellow arrow indicates the anterior (a-lineage) expression of Gsx while turquoise arrow indicates the posterior (A-lineage) domain of Gsx,*

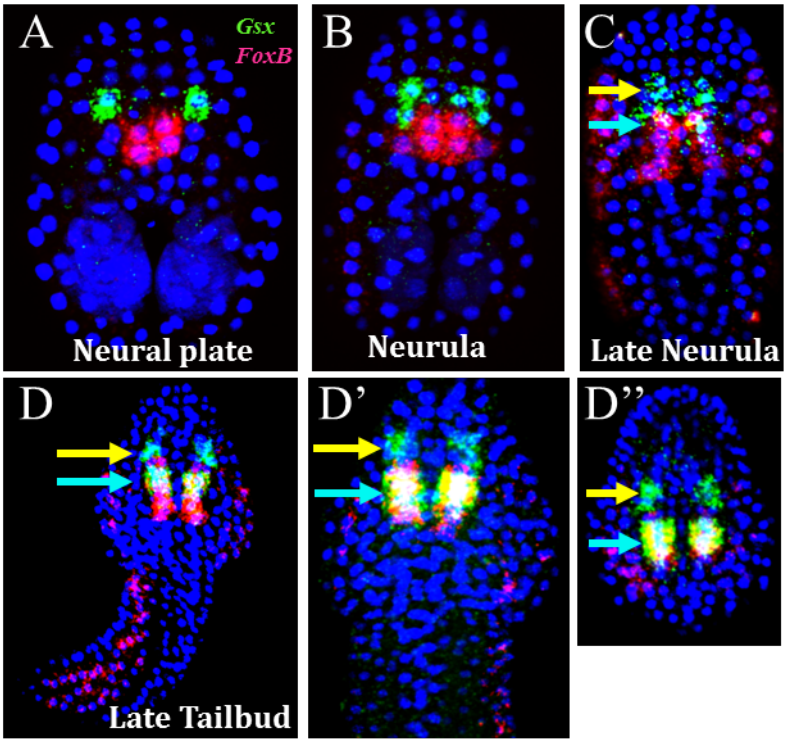

Fig. 3.10 Positional relationship of Gsx and FoxB gene expression. *Merged images, all in dorsal view, of double*

WMISH, plus DAPI nuclear staining (in blue), at different embryonic stages, reported on the bottom of each picture row. D' and D'' are enlarged and more dorsal images of D. Yellow arrow, in C, D, D', D'', indicates the anterior (a-lineage) expression of Gsx while turquoise arrow indicates the posterior (A-lineage) domain of Gsx, which overlaps with the anterior domain of FoxB,

3.2.1 *pGsx* reporter genes to label derivatives of *Gsx* expressing blastomeres at the larval stage

As previously reported, the signal from *Gsx* endogenous transcript is not detectable at the larval stage. To clarify if *Gsx* expression labels the precursors of larval photoreceptor cells, my research strategy involved the detection of fluorescent reporters downstream of the *2.8*Kb cis-regulatory region of *pGsx* (*pGsx>mCherry*) previously identified in the Lab. Indeed, *pGsx>mCherry* construct (as the other *pGsx* constructs used in this study), thanks to the stability of the fluorescent protein product, is able to recapitulate endogenous gene expression up the larval stage, when a strong signal is clearly detectable in the presumed photoreceptor cells territory. A further signal is often visible also in the ventral part of the sensory vesicle (Fig. 1.11, G, H).

It is important to remark that the slight variations in the territories expressing mCherry among different embryos are in agreement with the mosaic incorporation of transgenes in ascidians, in the sense that after a variable number of cell divisions, the exogenous plasmid might segregate into both or only one of the 2 daughter cells originating from a single precursor. Depending on the number of cell divisions, a variable number of cells within a tissue will come to lack the transgene.

For double electroporation experiments I exploited also *pGsx>GFP* and *pGsx>H2BmCherry* constructs, the last labelling specifically the nuclei of the transgenic cells thanks to the presence of the Histone 2B domain.

3.2.2 pGsx labels PRCs territories at the larval stage

To test if *pGsx* could effectively drive the expression of the reporter gene in photoreceptor territories at the larval stage, double electroporation experiments were performed using *pGsxH2B>mCherry* in

combination with *pArr>eGFP*, which labels specifically larval photoreceptor cells (Yoshida et al., 2004). The results were comparable between several independent experiments and the percentage of larvae showing both signals was more than 90%. The expression of the reporters was checked at different developmental stages and only from late tailbud/initial larval stage the *pArr>eGFP* driven signal became evident (Fig. 3.3 A, B) and was detected in a subpopulation of *pGsxH2B>mChe* fluorescent cells (yellow areas). The co-expression persisted and, in most cases, become even stronger at the larval stage, showing that pGsx labels a population of neural cells, which includes the *pArr* expressing cells.

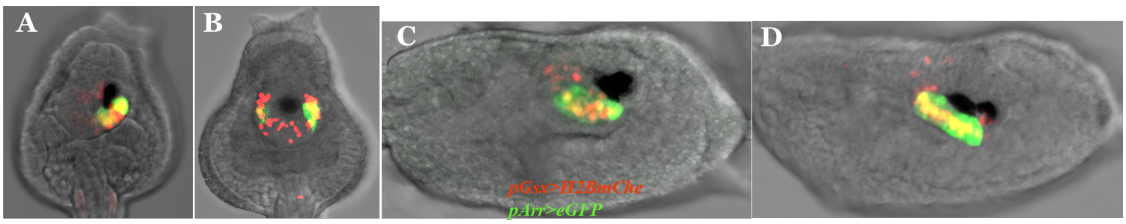

Fig. 3.11 Confocal imaging of *pGsx>H2BmCherry* + *pArr>eGFP* constructs. Merged images, in dorsal (A, B) and lateral (C, D) view. Overlapping territories result in yellow areas.

3.2.3 Photoreceptor territories: A-lineage or a-lineage?

My data indicates that *pGsx* is able to guide the expression of the reporter gene in some areas of the CNS, including photoreceptor territories. On the other hand, *Gsx* transcript labels both A-lineage and a-lineage during embryogenesis. In the attempt to gather further information on the contribution of a/A-lineages to photoreceptor cells formation, I performed a number of double electroporation experiments, exploiting *pArr>eGFP* in combination with: *pDMRT>H2BmCherry* (or *pDMRT>H2BYFP*), which drive reporter expression in a-lineage neural plate derivatives (Wagner and Levine, 2012) or *pFoxb>H2BmCherry* (*pFoxB>H2BYFP*), which drives reporter expression in A-lineage neural plate derivatives (Imai et al., 2004).

Electroporation of *pArr>eGFP* + *pFoxb>H2BmCherry* constructs resulted in tailbud embryos and larvae showing overlapping fluorescent signals in a wide area that in some cases did not include the

most anterior Arrestin positive territory (Fig. 3.4).

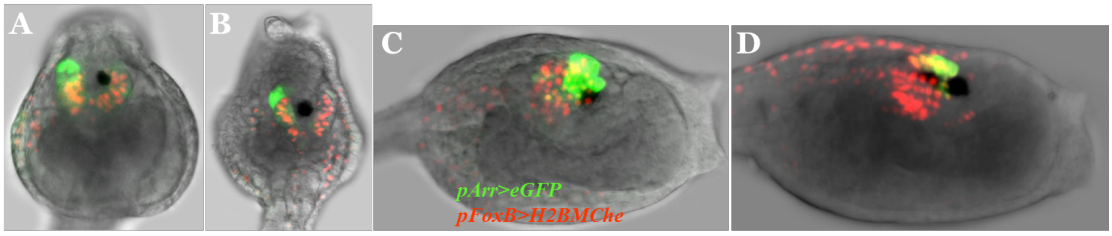

***Fig. 3.12 Confocal imaging** of **pFoxb**>H2BmChe + **pArr**>eGFP **constructs**. Merged images, in dorsal (A, B) and lateral (C, D) view. Overlapping territories result in yellow areas.*

Electroporation of *pArr>eGFP + pDMRT>H2BmCherry* constructs resulted in tailbud embryos and larvae with the overlapping signal present in a small area often localized at the level of anterior Arrestin positive cells (Fig. 3.5).

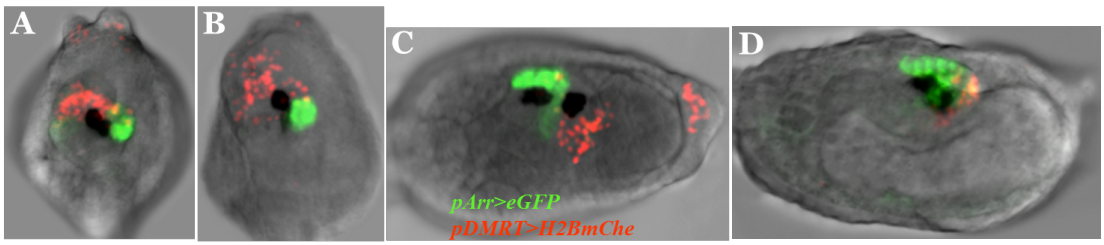

***Fig. 3.13 Confocal imaging of pArr**>eGFP + **pDMRT**>H2BmChe **constructs**. Merged images, in dorsal (A, B) and lateral (C, D) view. Overlapping territories result in yellow areas*

Thus, my double electroporation experiments, while confirming that the bulk of photoreceptor cells of the ocellus are A-lineage derived, as recently inferred (Oonuma et al., 2016), suggest that also a-lineage, with a small number of cells, could participate in the organization of this structure.

In parallel, the same approach was used to explore the localization, in photoreceptor territories at the larval stage, of the progeny of a- and A-lineage blastomeres expressing *Gsx*. To this end, I performed double electroporation experiments, exploiting *pGsx>GFP* (or *pGsx>H2BmChe*) in combination with: *pDMRT>H2BmCherry* (or *pDMRT>H2BYFP*), or *pFoxb>H2BmCherry* (or *pFoxB>H2BYFP*).

In a series of experiments I tested the probable contribution of a-lineage *Gsx* expressing blastomeres to the formation of PRCs by co-electroporating *pGsx>eGFP* plus *pDMRT>H2BmCherry* and analyzed the embryos from the late-taibud stage. In most of the specimens analyzed in this study, I observed that the signals of mCherry and GFP overlap in the *Gsx* anterior domain of "photoreceptor territories" which corresponds to the more-posterior area of DMRT positive region. This co-localization persisted up to the larval stage (Fig. 3.6).

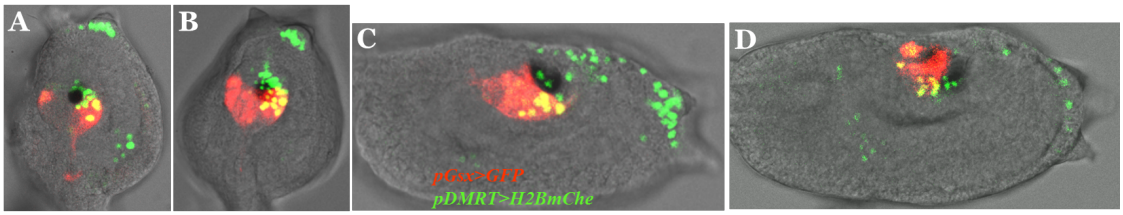

Fig. 3.14 Confocal imaging of pGsx>GFP + pDMRT>H2BmChe constructs. *Merged images, in dorsal (A, B) and lateral (C, D) view. Overlapping territories result in yellow areas.*

Co-electroporation of *pGsx>H2BmCherry* plus *pFoxB>H2BYFP* transgenes resulted instead in tailbud embryos showing a co-localization of fluorescent signals in the posterior region of *Gsx* "photoreceptor territories" (Fig. 3.7). The overlap of the two signals persisted up to the larval stage.

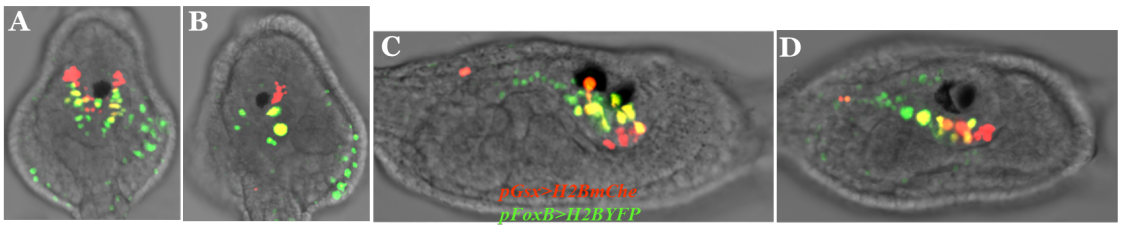

Fig. 3.15 Confocal imaging of pGsx>H2BmChe + pFoxB>H2BYFP constructs. *Merged images, in dorsal (A, B) and lateral (C, D) view. Overlapping territories result in yellow areas.*

This part of my work permitted to get insights on the contribution of a/A-lineage to *Gsx* expression in the "presumed photoreceptor territories" from late-tailbud up to the larval stage.

3.2.4 Concluding Remarks

The revised lineage of larval photoreceptor cells in *Ciona*, by Oonuma et al. (Oonuma et al., 2016), is consistent with the photoreceptor cell lineage reported in another ascidian species, *Halocynthia roretzi* (Taniguchi and Nishida, 2004). It is interesting to note that in *Halocynthia* the authors claim that the Hrarr-positive region almost precisely match the region derived from A8.7R (right) (the progenitor of A9.14) blastomeres. However, they also highlight that "descendant cells of a8.17R (Right), which are progenitor of a9.33, were mixed with those of A8.7R, and the position of each descendant cell varied among specimens. This indicates that precise positions of the descendant cells are not deterministic at the clonal boundary between a8.17R and A8.7R, and that intercalation occurs between a8.17R and A8.7R derivatives "to some extent". In line with this, in my experiments I just noticed that the few a-lineage/Arrestin overlapping cells were undoubtedly mixed with other cells and, although preferentially positioned in the most anterior "photoreceptor territories", showed variable location in this region.

Thus, even if the majority of photoreceptor cells derive from A-lineage I cannot exclude that, based on my data, a small contribution is also provided by a-lineage cells. In this regard, as previously reported, *Ciona* photoreceptor cells fall into three main classes I, II and III, with the first two of these constituting the 30 known ocellus pigment cup associated photoreceptors, 18-23 in group I and 7-11 in group II. The outer segments of group I are arranged in rows inside the pigment cup while outer segments of group II photoreceptors occur anterior to the pigment cup, within the lumen of the brain vesicle (Horie et al., 2008b). Recently Ryan et al. have studied, by means electron microscopy, thin sections from the brains of *Ciona* larvae to analyze their connectome (Ryan et al., 2016). This study revealed that the group II comprises seven most anterior PRCs that project outer segments directly into the lumen of the SV. They are in contact with lens cells and extend axons toward the posterior brain vesicle along the main photoreceptor axon tract, on the right ventral border of the CNS. There are two rows of these type II photoreceptors, one row of three photoreceptors (Type II-i) anterior to

the pigmented portion of the ocellus pigment, and another row of four (Type II-ii) photoreceptors located more posteriorly. Type I photoreceptors lie adjacent to the Type II photoreceptors on the dorsal right side, but extend their outer segments into the ocellus pigment cup. These Type I photoreceptors are grouped in five rows (I-i to I-v) of 5, 5, 4, 4, and 5 cells respectively and it seems that most of them (I-i, I-ii, I-iii, I-iv) express reporters for glutamate, whereas II-i, II-ii, and possibly I-v express reporters for GABA (Horie et al., 2010; Horie et al., 2008b; Ryan, 2016). This ultrastructural analysis revealed also the connections between the photoreceptors (Ryan, 2016; Ryan et al., 2016). All layers appear to be fully connected. Anatomically strongest interactions amongst rows of photoreceptors are bidirectional between Type I-i and I-iv, I-i and I-iii, and I-i and I-v. In contrast, Type II photoreceptors receive input from both Types I-iv and I-v. At the level of light perception and neurotransmitter action, when light is off, the glutamatergic photoreceptors reinforce each other's release of glutamate, whereas a "light on" response prevent the release of glutamate by all photoreceptors. If Type I-v and Type II photoreceptors are GABAergic, and still hyperpolarize to light, then they should inhibit their photoreceptor targets, which express GABA receptors according to Zega et al. (Zega et al., 2010). Thus the new scenario, emerged from this exhaustive study, indicates that not all the PRCs have the same role in perceiving and transmitting light inputs. Furthermore, even considering the simplicity of *Ciona* ocellus, the signals generated from light perception are integrated thanks to the cross talk between the different types of PRCs, before being transmitted to the posterior brain and to the visceral ganglion, in order to generate the proper muscle contraction.

It is interesting to note that the type II PRCs, about 7 in number and the anterior-most PRCs, are GABAergic, while type I PRCs about 23, and located more posteriorly are most Glutamatergic.

It is tempting to speculate that these different characteristics could be related to different lineage origins, with type II generated by a-lineage and type I originated by A-lineage. On these grounds, we have just planned to check this hypothesis by doing double immuno experiments on transgenic

pDMRT>H2BmChe, *pFoxB>H2BmChe* or *pGsx>H2BmChe* larvae using mCherry and either GABA or Glutamate antibody.

Concerning *Gsx*, the data collected in this part of my study indicate that *Gsx*, in spite of the recent lineage revision, remains a good marker of photoreceptor cells given its expression from neural plate stage in a-lineage, which labels the "old" photoreceptor precursors, and its next activation, at the neurula stage, in the A-lineage, which includes the "new" photoreceptor precursors. Based on these new findings, we have planned to further refining the previous studies, done by the former PhD student Rosaria Esposito, on *Gsx* activity in photoreceptor formation. Our analysis will include the effects exerted by targeted perturbation of the endogenous *Gsx* function, obtained by expressing constitutively active and repressive forms of *Gsx*, on endogenous Arrestin expression and on the activity of Arrestin promoter at the larval stage. The aim is to further supporting previously collected evidences on the involvement of *Ciona Gsx* in the developmental programs leading to photoreceptor cells differentiation, which opens new perspectives about the function of this transcription factor in nervous system formation during evolution.

3.3 Behavioural tests on *Ciona* larvae

Even simpler organisms are able to respond to diverse environmental stimuli, including the hydrostatic pressure that increases with dept. For a free-swimming animal, it is essential to be spatially placed at the correct depth. As regard to *Ciona*, still little is known about a "pressure response" and the sole study on this subject (Tsuda et al., 2003b) suggests that pressure increase does not affect larval swimming. However, this issue needs to be further investigated, since it is difficult to imagine that a free-swimming animal, even if evolutionary simple, is unable to detect a force acting on its body. In the last part of my PhD studies, my efforts were thus devoted to setting a series of texts in order to detect any behavioral modification of *Ciona* specimens, at different developmental larval stages, subjected to the increase of one bar of hydrostatic pressure. To this end, I spent 3

months in Gáspar Jékely lab, at the Max Planck Institute for developmental biology, working in collaboration with Dr. Luis Bezares.

3.3.1 Does *Ciona* larva respond to pressure variations?

In a first series of tests, *Ciona* larvae were analyzed 30' after hatching in three independent experiments. Larvae were moved to the pressure chamber 6 times at 1h-intervals (5 hours total). For each test, their swimming behavior was analyzed and recorded for a time window of 4 minutes, after which the larvae were placed back in the glass beaker at 18°C. This analysis indicated that the animals seem to respond to 1 bar hydrostatic pressure increase by swimming quickly upwards, in the time window of 1,5h post hatching (Fig. 3.8). At later stages of larval development, this response was not more appreciable.

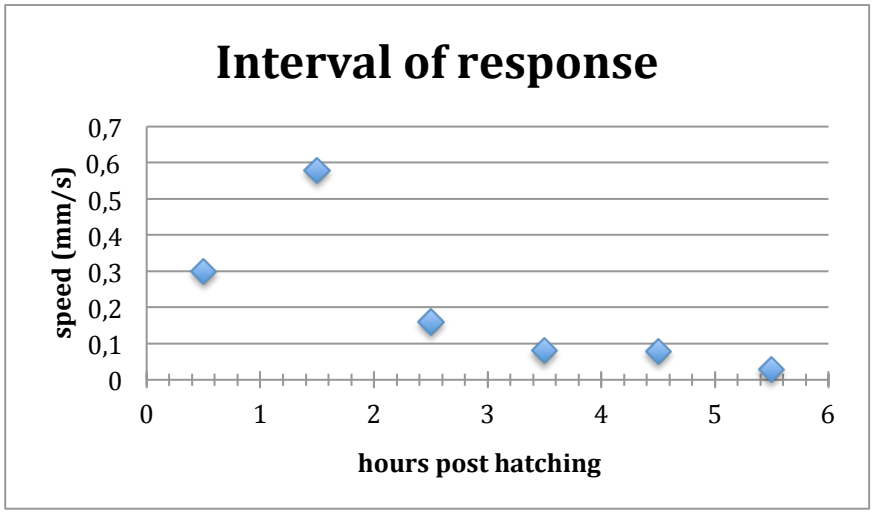

Fig. 3.16 Response of Ciona larvae to pressure increase. *The plot shows speed of animal recorded from 30' after hatching at 1h interval. The recording schedule is divided in 30s no pressure, 90 seconds pressure increase of 1 bar and then 30 seconds pressure release. The maximum speed is 0,58mm/s at the 1,5h time point. Then the response rapidly decreases.*

3.3.2 Pressure behavior characterization

The results of six independent experiments, aimed at further and better defining the hydrostatic pressure response, showed that a consistent subset of larvae, 1,5h post-hatching, swim faster upward at 1 bar pressure increase into the chamber. The speed extrapolated from the video recording reaches

an average maximum around 0,6mm/sec (Fig. 3.9). The observed behavior thus indicates that *Ciona* larvae are able to perceive and respond to hydrostatic pressure changes. Moreover, larvae stop swimming and start to sink as soon as the stimulus is finished.

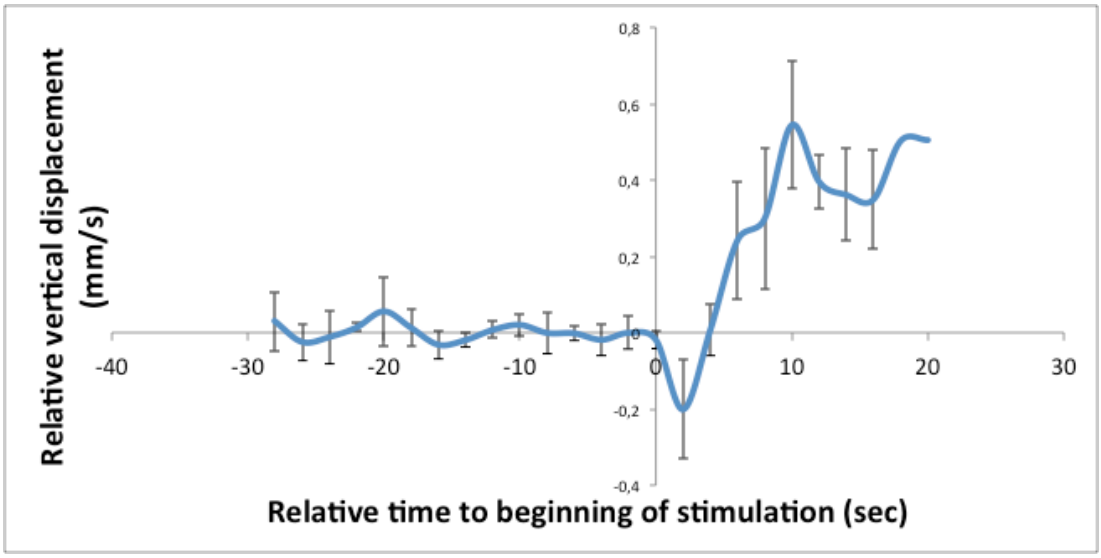

Fig. 3.17 Pressure behavior characterization. *The plot describes the speeds recorded from six independent w.t. batches exposed to 1 bar pressure increase. The recording schedule is divided in 30 seconds no pressure, 90 seconds pressure increase of 1 bar and then 30 seconds pressure release. The larvae were exposed to pressure increase at time 0. The animals started to swim faster toward surface soon after the stimulation.*

3.3.3 Looking for structures involved into hydrostatic pressure response

In the attempt to identify which structure could be involved in the detection of pressure increase, my attention was focused on the coronet/dopaminergic cells. To this end I prepared the *pTH>GCaMP* construct, in which the coronet/dopaminergic cells specific *Tyrosine Hydroxylase* (*TH*) promoter (Moret et al., 2005a), available in the Laboratory, was cloned upstream of the *GCaMP* reporter (genetically encoded calcium indicator).

GCaMPs are engineered proteins that contain Ca2+ binding motifs within a circularly permuted enhanced green fluorescent protein (eGFP) and are used to monitor intracellular Ca2+ rising by detecting any increase in fluorescent emission from eGFP. The calcium influx is considered the key

marker of a neuronal activation, since calcium is necessary to receive and transmit the signal toward other neurons. In a first set of experiments I simply observed under confocal microscope double transgenic *pTH>GCaMP/pTH>H2BmCherry* larvae, 1,5h post-hatching. In these and in the next experiments *pTH>H2BmCherry* transgene was used in combination with *pTH>GCaMP* in order to better identify and focus the region to be analyzed, given that the fluorescent signal emitted by mCherry protein is more stable compared to the fluctuating signal emitted by GCaMP protein.

Unexpectedly, during the observation of *pTH>GCaMP* transgenic larvae under confocal microscope, I detected and recorded an increase and decrease of the fluorescent signal, thus indicating a potential activity in these cells, induced by…. which stimulus? (Fig. 3.10).

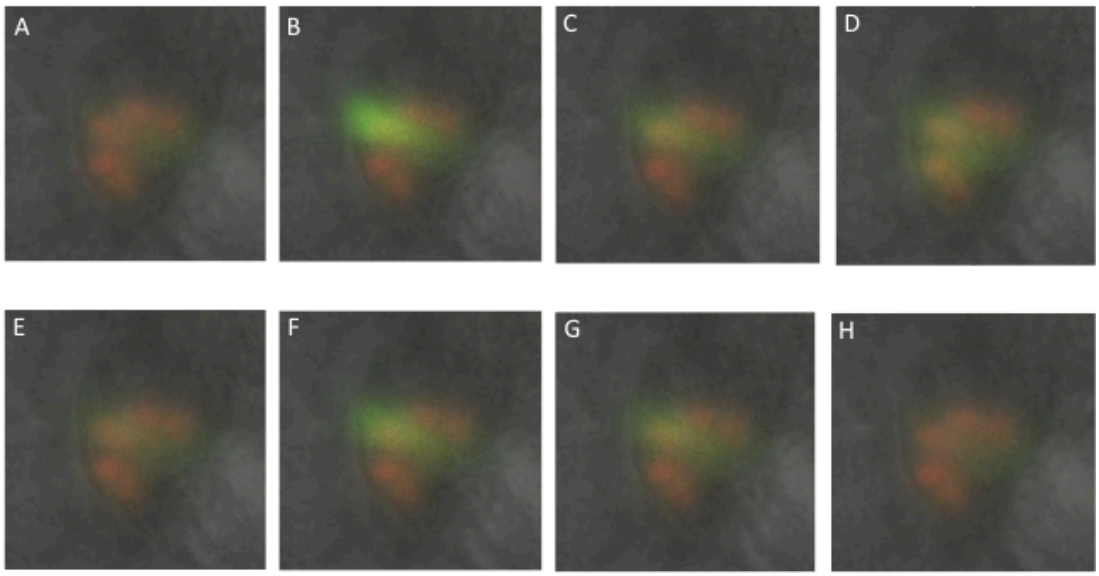

Fig. 3.18 GCaMP activity in transgenic larvae. *The figures are extrapolated from the in-vivo recording of a double electroporated (pTH>GCaMP/pTH>H2BmCherry) larva. In (A, E and H) the green fluorescence is at basal level, while in (B,C,D,F and G) is evident an increase of fluorescent signal. This indicates that GCaMP fusion protein is detecting neuronal spykes triggered by calcium influx induced by a stimulus. The animal in this experiment was not exposed to pressure increase.*

3.3.4 GCaMP as tool to monitor neuronal activity in *Ciona* larvae

I then tested if the pressure stimulation could further affect neuronal activity of coronet cells. To this end, I carried out in vivo experiments, by exposing double transgenic *pTH>GCaMP* + *pTH>H2BmCherry* larvae, 1,5h post-hatching, to 1 bar hydrostatic pressure increase.

Transgenic *pTH>GCaMP/pTH>H2BmCherry* larvae were first selected at 18hpf looking for mCherry signal positivity (the mCherry+ embryo percentage was around 95%) and then singularly checked under confocal microscopy. Positive larvae were glued singularly by the tail on a cover slip and then placed in a special chamber in which it is possible to apply increased pressure. This chamber has been designed by dr. Bezares and fits under the confocal microscope. The in vivo recordings were done in the time window of 1,5h post hatching under the confocal microscopy, by a Z-stack scan of the GCaMP positive area. Three independent experiments were performed. The experimental design consisted in two subsequent rounds of Z-stack recording: 30 seconds prior, 30 seconds 1 bar pressure increase and 30 seconds post increase pressure removal.

The analysis of about 10 larvae, from three rounds of experiments, indicated that GCaMP intensity does not change in response to pressure (Fig. 3.11, 3.12, 3.13). The only noticeable change was present in the third experiment during the "second round of pressure increase" (Fig. 3.13 D,E), but this is unlikely to consider it as a "pressure response" since it lasted also in the "post increase" period. Maybe this intensity change was triggered by other stimuli, probably light stimuli, since the animal was subjected to laser illumination.

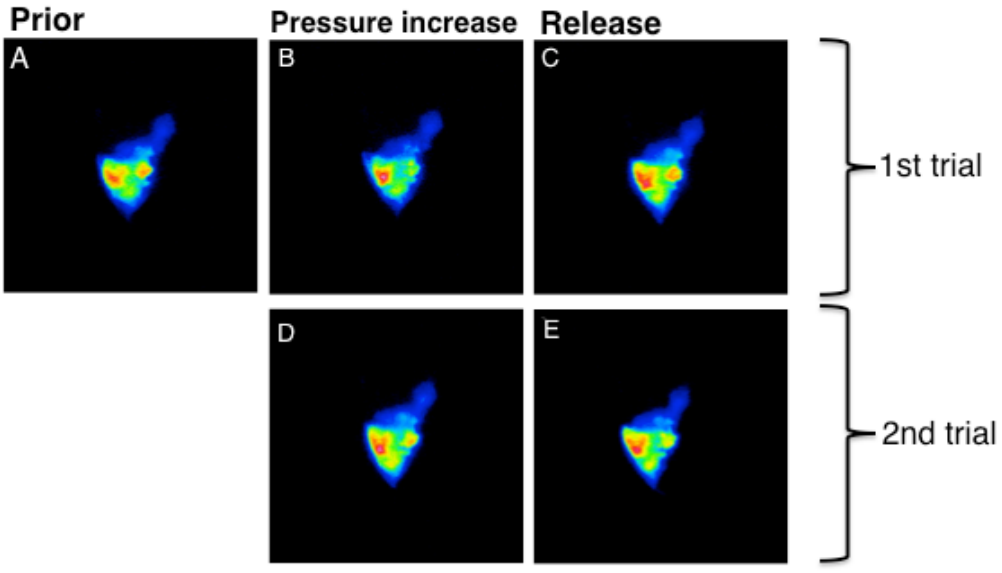

Fig. 3.19 In the images are displayed the fluoresce intensities of pTH>GCaMP electroporated animals. In vivo z-scan analysis of larvae in three conditions: prior to pressure stimulation (A), 1bar pressure increase (B and D) and pressure release (C and E). The intensities do not change among different experimental condition.

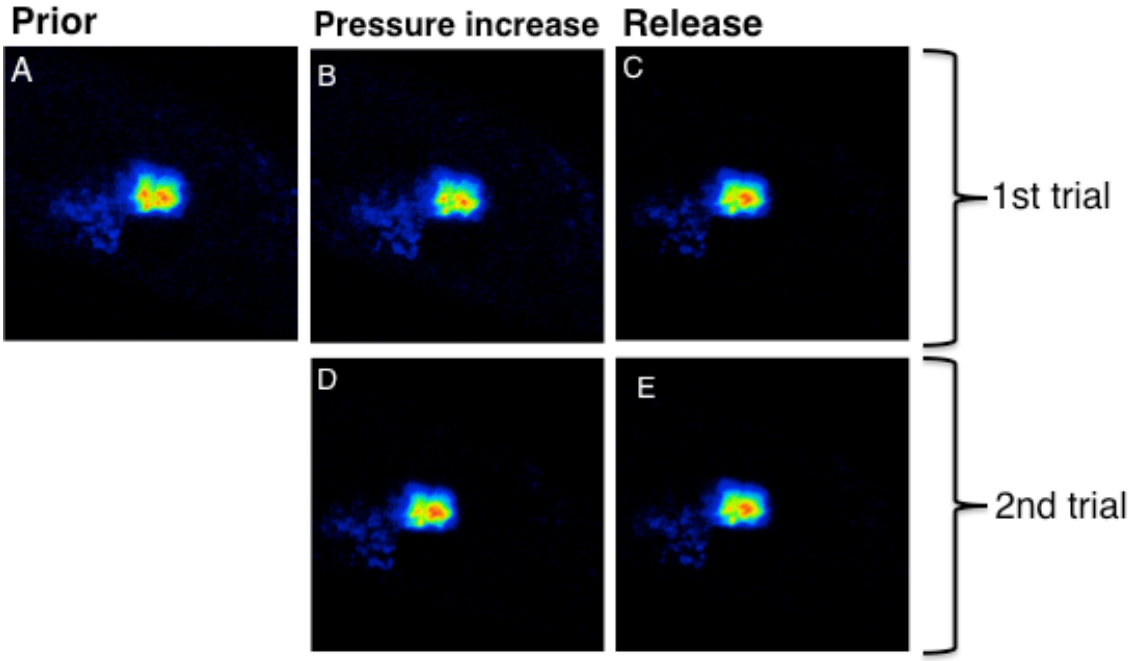

Fig. 3.20 In the images are displayed the fluoresce intensities of second indipendent pTH>GCaMP experiment. In vivo z-scan analysis of larvae in three conditions: prior to pressure stimulation (A), 1bar pressure increase (B and D) and pressure release (C and E). The intensities do not change among different experimental condition.

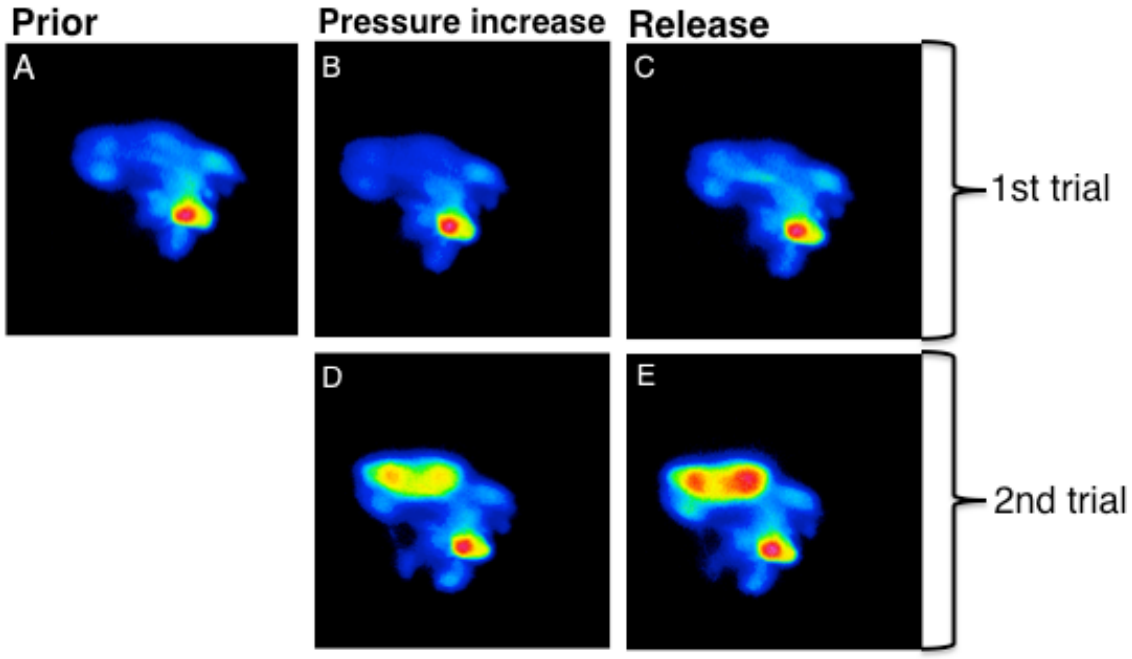

Fig. 3.21 In the images are displayed the fluoresce intensities of third electroporation pTH>GCaMP experiment. In vivo z-scan analysis of larvae: prior to pressure stimulation (A), 1bar pressure increase (B and D) and pressure release (C and

E). An increase of fluorescence can be observed in second pressure stimulation (D), but the signal is unlikely to be related to pressure perception because, in (E) the intensity of fluorescent signal appear even stronger.

3.3.5 Concluding Remarks

My results, even if preliminary and to be further investigated, indicate the presence of a "pressure-behavior" in *Ciona* larvae, thus contradicting, for some aspects, the previous findings by Tsuda (Tsuda et al., 2003b). Actually, I conducted a detailed analysis within a wide time window, by screening larval behavior at different developmental times after hatching. This approach permitted to verify that animals display a pressure-related behaviour within a maximum of 1,5 h post hatching. Then the response becomes weaker soon after this developmental window. In Tsuda's study, the larvae were instead examined from 3h post hatching. Thus, the absence of a pressure response in their experiments could be related just to the developmental stage they choose to analyze this behavior, 3 h post-hatching, while my data clearly indicate that the pressure response occurs a maximum of 1,5 h post hatching. Moreover, they used a different recording chamber. The chamber used in my experiments, developed by Dr Bezares, is bigger (width×depth×length=25·mm×100·mm×70·mm) than the optical quartz cell (width×depth×length=10·mm×40·mm× 10·mm) used by Tsuda. Probably the recording in a bigger chamber permitted a more accurate tracking of larval movement. Moreover, in the pressure chamber I used, the air increase apparatus is included in the lid, which is tightly screwed to the rest of the chamber. This design provide a uniform pressure increase and prevent pressurized air to be dispersed. This latter expedient could cooperate to increase the overall reliability of the results.

Another interesting outcome of the work is that the in vivo calcium imaging reporter, GCaMP, functionally active in *Ciona,* can be added to the myriad of tools yet available for this model system and will be very useful in future analyses. Indeed, thanks to the outstanding work done by Ryan et al. (Ryan et al., 2016), aimed at unveiling *Ciona* connectome, a lot of neuronal circuits have been revealed. One can suppose that, by expressing GCaMP in specific neuronal lineages, it will be

possible to carry out anatomical and, at the same time, functional analyses of individual neuronal circuits.

Concerning coronet cells, even if still preliminary, the result tend to exclude their involvement in hydrostatic pressure perception, in line with the results proposed by Tsuda et al. (Tsuda et al., 2003b). About this subset of cells, Moret (Moret et al., 2005a) proposed that they could be functionally active from the late larval stages up to the beginning of metamorphosis. Indeed, the onset of DA biosynthesis and the growth of the DA-positive axons occur few hours after hatching, and DA immunoreactivity is no longer detected in metamorphosing specimens. On these grounds, it has been postulated (Moret et al., 2005a) that the late DA synthesis onset could contribute to the age-dependent changes in the swimming behavior of larvae (Tsuda et al., 2003a; Tsuda et al., 2003b). This role is supported by the evidence that dopaminergic neurons send projections to the posterior region of the sensory vesicle controlling locomotion. Indeed, this region contains cholinergic and GABAergic cells, which send axons to the visceral ganglion, where motoneurons are localized (Yoshida et al., 2004).

Coronet/dopaminergic cells, as previously reported, are located near the type III photoreceptor cells, supporting a role in the modulation of photic response (Razy-Krajka et al., 2012). Thus the function of coronet/dopaminergic cells could be integrated in the visual circuit, and in line with this one can suppose that the activation I detected during the observation of *pTH>GCaMP* transgenic larvae under confocal microscope (Fig. 3.10) may have been triggered by laser illumination.

As future perspective of this work, we have already planned the preparation of a number of constructs in which GCaMP will be placed under pan neuronal promoter and lineage specific promoters, in order to identify which subset of neuronal cell is able to detect the hydrostatic pressure changes and guide the behavioral response that I revealed in my tests.

Bibliography

Esposito, R., Yasuo, H., Sirour, C., Palladino, A., Spagnuolo, A., Hudson, C., 2017. Patterning of brain precursors in ascidian embryos. Development 144, 258-264.

Horie, T., Nakagawa, M., Sasakura, Y., Kusakabe, T.G., Tsuda, M., 2010. Simple motor system of the ascidian larva: neuronal complex comprising putative cholinergic and GABAergic/glycinergic neurons. Zoolog Sci 27, 181-190.

Imai, K.S., Hino, K., Yagi, K., Satoh, N., Satou, Y., 2004. Gene expression profiles of transcription factors and signaling molecules in the ascidian embryo: towards a comprehensive understanding of gene networks. Development 131, 4047-4058.

Oonuma, K., Tanaka, M., Nishitsuji, K., Kato, Y., Shimai, K., Kusakabe, T.G., 2016. Revised lineage of larval photoreceptor cells in Ciona reveals archetypal collaboration between neural tube and neural crest in sensory organ formation. Dev Biol 420, 178-185.

Pasini, A., Amiel, A., Rothbacher, U., Roure, A., Lemaire, P., Darras, S., 2006. Formation of the ascidian epidermal sensory neurons: insights into the origin of the chordate peripheral nervous system. PLoS Biol 4, e225.

Rothbacher, U., Bertrand, V., Lamy, C., Lemaire, P., 2007. A combinatorial code of maternal GATA, Ets and beta-catenin-TCF transcription factors specifies and patterns the early ascidian ectoderm. Development 134, 4023-4032.

Ryan, K., 2016. The connectome of the Larval Brainof Ciona intestinalis (L.).

Shimai, K., Kitaura, Y., Tamari, Y., Nishikata, T., 2010. Upstream regulatory sequences required for specific gene expression in the ascidian neural tube. Zoolog Sci 27, 76-83.

Taniguchi, K., Nishida, H., 2004. Tracing cell fate in brain formation during embryogenesis of the ascidian Halocynthia roretzi. Dev Growth Differ 46, 163-180.

Tsuda, M., Kawakami, I., Shiraishi, S., 2003a. Sensitization and habituation of the swimming behavior in ascidian larvae to light. Zoolog Sci 20, 13-22.

Wagner, E., Levine, M., 2012. FGF signaling establishes the anterior border of the Ciona neural tube. Development 139, 2351-2359.

Zega, G., Candiani, S., Groppelli, S., De Bernardi, F., Pennati, R., 2010. Neurotoxic effect of the herbicide paraquat on ascidian larvae. Environ Toxicol Pharmacol 29, 24-31.